

AD-A033 434

FLORIDA UNIV GAINESVILLE ENGINEERING AND INDUSTRIAL--ETC F/G 17/9
FM RANGING USING A FREQUENCY REACTION CORRELATOR.(U)

OCT 76 M C BARTLETT, R C JOHNSON, L W COUCH DAAG39-76-C-0043

HDL-CR-76-043-1

NL

UNCLASSIFIED

|OF|

AD
A033434



END

DATE
FILMED
2-77

NDL-CR-76-043-I

12

FM RANGING USING A FREQUENCY REACTION CORRELATOR

October 1976

ADA033434

FM Ranging using a Frequency Reaction Correlator, by Malcolm G. Johnson and Levo W. Czech

Prepared by

Engineering and Industrial Experiment Station
College of Engineering
University of Florida
Gainesville, Florida 32611

Under Contract

DAAG39-76-C-0043

DDC
REF ID: A60000
REGISTERED



U.S. Army Materiel Development
and Readiness Command
HARRY DIAMOND LABORATORIES
Adelphi, Maryland 20783

The findings in this report are not to be construed as an official Department of the Army position unless so designated by other authorized documents.

Citation of manufacturers' or trade names does not constitute an official endorsement or approval of the use thereof.

Destroy this report when it is no longer needed. Do not return it to the originator.

UNCLASSIFIED

SECURITY CLASSIFICATION OF THIS PAGE(When Data Entered)

modulated oscillator due to an injected signal is developed. Possible applications of the Frequency Reaction Correlator include doppler ranging, directional doppler ranging, and remote sensing or telemetering. A digital technique for implementing the Frequency Reaction Correlator is discussed. Mathematical analyses and experimental data are presented and are shown to be in agreement.




TABLE OF CONTENTS

1. INTRODUCTION 5

2. REACTION OF A FREQUENCY MODULATED OSCILLATOR TO INJECTED SIGNALS . . 6

 2.1 General Oscillator Reaction Phenomena 6

 2.2 Oscillator Reaction To Targets 8

3. FREQUENCY REACTION CORRELATOR 10

4. SYSTEM APPLICATIONS 18

 4.1 Doppler Ranging 19

 4.2 Directional Doppler Ranging 19

 4.3 Remote Sensing 20

5. SYSTEM SIGNAL AND NOISE CONSIDERATIONS 26

 5.1 Target Signal Amplitude 26

 5.2 System Signal/Noise Ratios 27

6. SYSTEM IMPLEMENTATION CONSIDERATIONS 29

 6.1 Functional Requirements 29

 6.2 RF Delay Line/Mixer Implementation 30

 6.3 Digital Delay Line/Mixer Implementation 30

 6.3.1 Operating Principles 30

 6.3.2 Mathematical Analysis 34

 6.3.3 Test Results 36

7. CONCLUSIONS 39

SELECTED BIBLIOGRAPHY 40

APPENDIX A--Attenuation Factor Caused By Phase Shift Of The Oscillator
 Reaction By The Delay Line 41

DISTRIBUTION 45

ACCESSION NO.	
NTIS	<input checked="" type="checkbox"/>
DIC	<input type="checkbox"/>
UNANNOUNCED	<input type="checkbox"/>
JUSTIFICATION	
BY	
DISTRIBUTION AVAILABILITY CODES	
DIAL	AVAIL. REC. BY SPECIAL
A	

LIST OF FIGURES

1.	Frequency Modulated Oscillator	6
2.	Oscillator Reaction Patterns as a Function of Radian Difference-Frequency Between Injected and Carrier Frequencies	8
3.	Measured Oscillator Reaction With Strong Target-Triangle FM, $B\tau \approx 4\frac{1}{2}$	10
4.	Frequency Reaction Correlator	10
5.	$R(t, \tau)$ For a Very Strong Target Signal When $\tau \approx \tau_r$. Triangle FM, $B\tau_r \approx 5$	15
6.	Waveforms For $\tau_r = 0.08 \mu\text{sec}$	16
7.	Waveforms For $\tau_r = 0.18 \mu\text{sec}$	17
8.	Directional Doppler Ranging	19
9.	Directional Doppler Range Responses	20
10.	Directional Doppler Response For Sawtooth FM	22
11.	Directional Doppler Response For Triangle FM	23
12.	Directional Doppler Response For Sine Wave FM	24
13.	Directional Doppler Response For Triangle/Triangle FM/FM	25
14.	Remote Ranging System	26
15.	Power Spectrum of $n(t)\cos[\omega_c(t)\tau_r]$ for Narrow Band $n(t)$ Centered on Zero	28
16.	Digital Delay Line/Mixer System	31
17.	Theoretical Digital Delay Line/Mixer Waveforms	33
18.	Measured Responses for Digital Delay Line/Mixer $B\tau_r \approx 6.5$, $B = 20 \text{ MHz}$, $f_m = 10 \text{ KHz}$, Triangular Modulation	37
19.	Measured Range Response Illustrating Harmonic Range Responses	38
A-1.	Delay Line Correlator	41
A-2.	Attenuation Due to Phase Shift of Oscillator Reaction by Delay Line For Sawtooth FM	42

1. INTRODUCTION

A new type of IF correlator, to be referred to as the "Frequency Reaction Correlator," is reported. Possible applications of the Frequency Reaction Correlator include doppler ranging systems, directional doppler ranging systems, and remote sensing or telemetering systems. The Frequency Reaction Correlator is distinguished by the fact that it detects and correlates an IF signal what results from the frequency reaction of a radiating frequency modulated oscillator due to a target. In contrast, the IF correlators described in the references cited process an IF signal which results from the amplitude reaction of the oscillator. (Detecting an IF signal by mixing the transmitted signal and the signal received from a target is equivalent to detecting the amplitude reaction (by envelope detection) of a compliant oscillator with a target present).

To predict the response of the Frequency Reaction Correlator, it was necessary to properly describe the amplitude and frequency reactions of the compliant, frequency modulated oscillator which result from an injected signal. Section 2 develops the oscillator mathematical model starting from the basic oscillator interaction studies of Huntoon and Weiss.¹ The model developed has proven useful in predicting both first and second-order effects of oscillator interaction experiments. The IF signal due to amplitude reaction predicted by the interaction model of Section 2 is generally the same as would be obtained by assuming that the IF signal is the result of envelope detecting the sum of the transmitted and received signals (additive model). For frequency reaction effects, the simple additive model is inadequate and the compliant oscillator model of Section 2 must be employed.

The Frequency Reaction Correlator is implemented by coupling the RF voltage from a compliant RF oscillator to an RF delay line and mixer. The doppler range response is obtained by doppler filtering the mixer output. Detection of the IF signal and correlation with the IF reference is simultaneously accomplished in the RF delay line/mixer hardware. The RF mixer inputs can be saturated, since frequency variations rather than amplitude variations are being detected. Processing of the oscillator signal to measure range at a position remote from the oscillator is possible, because the target response is present on the oscillator radiated signal. The range response at the remote processor is the same as would be obtained at the oscillator; moreover, the effects of space losses between the oscillator and remote processor can be removed by saturating the RF mixer.

The system was tested using a small frequency modulated loop oscillator. This oscillator is "compliant"; that is, it reacts in both amplitude and frequency to an injected signal. Several of the references cited describe IF correlators that used this oscillator. For these systems, an IF signal was developed by envelope detecting the RF loop voltage (which detects the amplitude reaction). The Frequency Reaction Correlator is very similar to these systems, differing principally in that the IF signal is developed by detecting

¹Huntoon, R.D. and Weiss, A., "Synchronization of Oscillators," Proceedings of IRE, December 1947, Volume 35, Number 12.

the frequency reaction of the oscillator. The range of applications of the Frequency Reaction Correlator is somewhat more limited than that for the IF correlators described in the references due to the RF delay line/mixer hardware implementation (Appendix A).

The following sections contain mathematical analyses and measured data that illustrate the operation of the Frequency Reaction Correlator. Since there was some question as to the availability of suitable RF delay lines, a digital delay technique was developed. The digital implementation of the Frequency Reaction Correlator is illustrated with block diagrams, measured responses, and supporting mathematical analyses.

2. REACTION OF A FREQUENCY MODULATED OSCILLATOR TO INJECTED SIGNALS

2.1 General Oscillator Reaction Phenomena

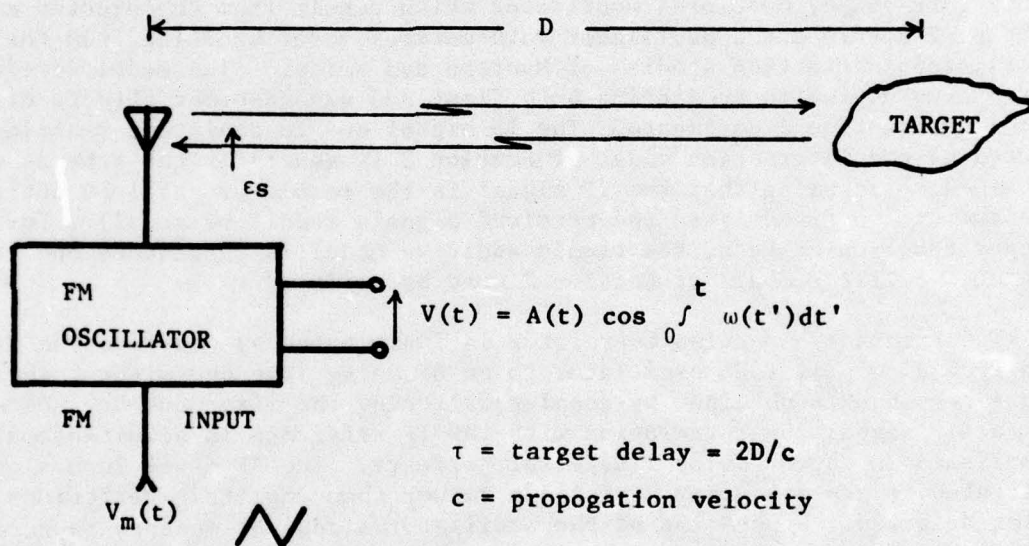


Figure 1. Frequency Modulated Oscillator

A radiating oscillator which receives either a small part of its radiation returned from a target or a signal from some other source is illustrated in Figure 1. The oscillator amplitude and frequency will react to the injected signal so that a voltage proportional to the oscillator voltage, $V(t)$, will be both amplitude and frequency modulated.¹ We will define the oscillator voltage, including the signal reaction effects, to be

$$V(t) = A(t) \cos \theta(t) \quad (1)$$

where $\theta(t) = \int_0^t \omega(t') dt'$.

¹Huntoon, R.D. and Weiss, A., "Synchronization of Oscillators," Proceedings of IRE, December 1947, Volume 35, Number 12.

The instantaneous amplitude and frequency variations of the oscillator are those due to its own deliberate modulation plus those due to the injected signal. Assuming a frequency modulated oscillator, these can be written as

$$\begin{aligned} A(t) &= A_0 + \Delta A(t) \\ \omega(t) &= \omega_c(t) + \Delta\omega(t) \end{aligned} \quad (2)$$

The oscillator frequency in the absence of injected signals is given by

$$\omega_c(t) = \omega_0 + \omega_m(t) = \omega_0 + DV_m(t), \quad (3)$$

where ω_0 is the center frequency and D is the deviation sensitivity in radians/volt.

The amplitude and frequency reactions are given by

$$\begin{aligned} \Delta A(t) &= a_s \cos [\phi_1(t) + \alpha] ; \\ \Delta\omega(t) &= \omega_s \cos [\phi_1(t) + \beta] . \end{aligned} \quad (4)$$

a_s and ω_s are the magnitudes of the reactions and $\phi_1(t)$ is the instantaneous phase difference between the injected signal and the oscillator voltage. The angles α and β are defined by the complex compliance coefficients of Huntoon and Weiss¹ and are dependent on the point where the oscillator voltage and injected signal are measured. For this reason, the individual values of α and β are not usually important whereas their difference, $\rho = \alpha - \beta$, is a parameter which defines the oscillator locking signatures. It is useful to modify (2) by substituting the relations

$$\begin{aligned} \phi_1(t) + \alpha &= \phi(t) \\ \phi_1(t) + \beta &= \phi(t) - \rho \end{aligned} \quad (5)$$

to obtain

$$\begin{aligned} A(t) &= A_0 + a_s \cos [\phi(t)] \\ \omega(t) &= \omega_c(t) + \omega_s \cos [\phi(t) - \rho] \end{aligned} \quad (6)$$

ρ is the phase angle between the amplitude and frequency reactions.

The magnitude of the amplitude and frequency reactions are directly proportional to the injected signal, which may be an incident signal field, an injected signal current, or an injected signal voltage. Assuming an incident field whose frequency falls within the tuned circuit response of the oscillator, the reactions can be written as

¹Huntoon, R.D. and Weiss, A., "Synchronization of Oscillators," Proceedings of IRE, December 1947, Volume 35, Number 12.

$$\begin{aligned}
 a_s &= K_a \sqrt{2} \epsilon_s \\
 \omega_s &= K_\omega \sqrt{2} \epsilon_s
 \end{aligned}
 \tag{7}$$

where ϵ_s is the rms field strength.

The coefficients K_a and K_ω must be determined by measurement of a_s and ω_s for a known injected signal level. A simple way to make these measurements is to radiate a constant amplitude field and measure the beat patterns produced by the oscillator reaction as this signal field is swept in frequency through the frequency of the unmodulated oscillator. These patterns are shown in Figure 2.



Figure 2. Oscillator reaction patterns as a function of radian difference-frequency between injected and carrier frequencies.

When the oscillator tank circuit approximates a high Q single-tuned circuit, $\rho = -\pi/2$, and the magnitudes of the amplitude and frequency reactions are related by²

$$\frac{\omega_s}{\omega_0} = \frac{a_s}{A_0} \cdot \frac{1}{2Q} = \frac{a_s}{A_0} \cdot \frac{\omega_t}{2\omega_0}
 \tag{8}$$

where ω_0 = oscillator center frequency,

and $\omega_t = \frac{\omega_0}{2Q}$ = oscillator tank bandwidth in radians/sec.

2.2 Oscillator Reaction To Targets

In (6), $\phi(t)$ is the phase difference between the injected signal and the oscillator voltage. If the signal is a delayed version of the transmitted waveform, $\phi(t)$ becomes

²Adler, Robert, "A Study of Locking Phenomena in Oscillators," Proceedings of IRE, June 1946.

$$\phi(t) = \int_{t-\tau}^t \omega(t')dt' = \int_{t-\tau}^t \omega_c(t')dt' + \int_{t-\tau}^t \omega_s \cos [\phi(t')-\rho]dt' , \quad (9)$$

where τ is the two-way propagation delay.

When the amplitude of the frequency reaction ω_s is small, the second order reaction effect (the second term in (9)) can be ignored and $\phi(t)$ becomes

$$\phi(t) = \int_{t-\tau}^t \omega_c(t')dt' . \quad (10)$$

For many ranging applications, $\phi(t)$ can be approximated by

$$\phi(t) \approx \omega_c(t)\tau . \quad (11)$$

The applicability of the results derived using (11) is discussed in Appendix A.

Assuming $\rho = -\pi/2$ and substituting (11) into (6) gives

$$\begin{aligned} A(t) &= A_0 + a_s \cos [\omega_c(t)\tau] ; \\ \omega(t) &= \omega_c(t) - \omega_s \sin [\omega_c(t)\tau] . \end{aligned} \quad (12)$$

These two equations may then be substituted into (1) to describe the oscillator voltage $V(t)$ when disturbed by its own returned signal. The model represented by (6) is more general than that represented (12) and has proven useful in predicting both first and second order phenomena observed in oscillator interaction experiments.

Equation (12) is verified by Figure 3 which illustrates the measured radian frequency $\omega(t)$ and amplitude reaction $a_s(t)$ of the oscillator in the presence of a very strong target when the oscillator is frequency modulated by a triangular wave. The number of beat cycles per sweep is given by the product of the peak-to-peak RF bandwidth B in Hz, and the time delay τ in seconds. For this case $B\tau = 4\frac{1}{2}$. If the target were not present, the measured frequency would be triangular and the amplitude reaction would be zero. It is evident that the amplitude reaction is not sinusoidal for the very strong target used for the illustration; however, most practical ranging applications will exhibit sinusoidal reactions since the targets will be much weaker.

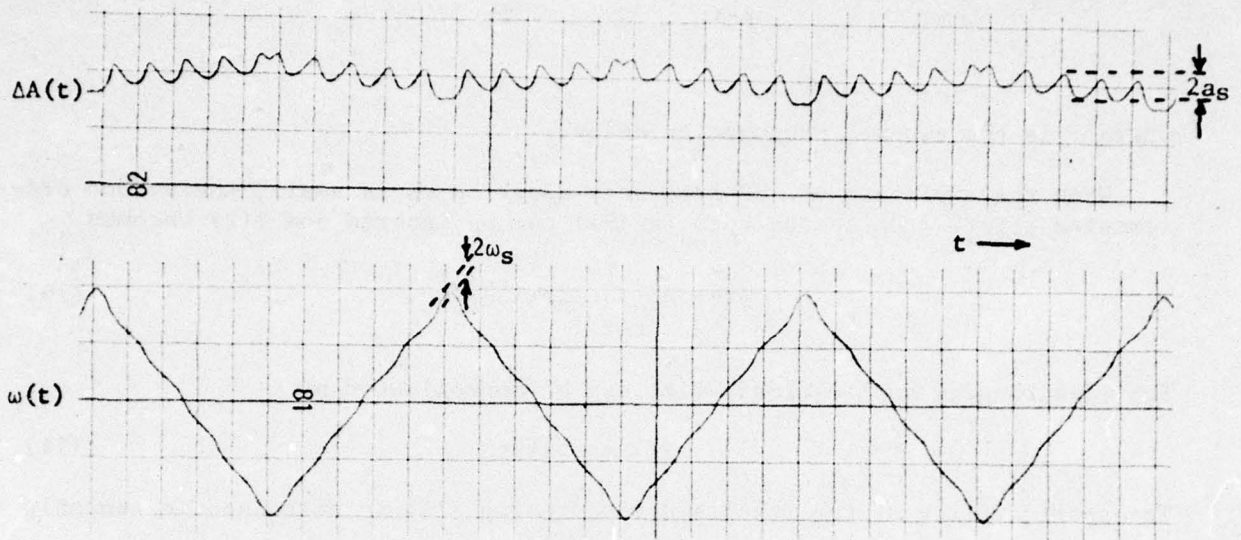


Figure 3. Measured oscillator reaction with strong target-triangle FM, $B\tau \approx 4\frac{1}{2}$.

3. FREQUENCY REACTION CORRELATOR

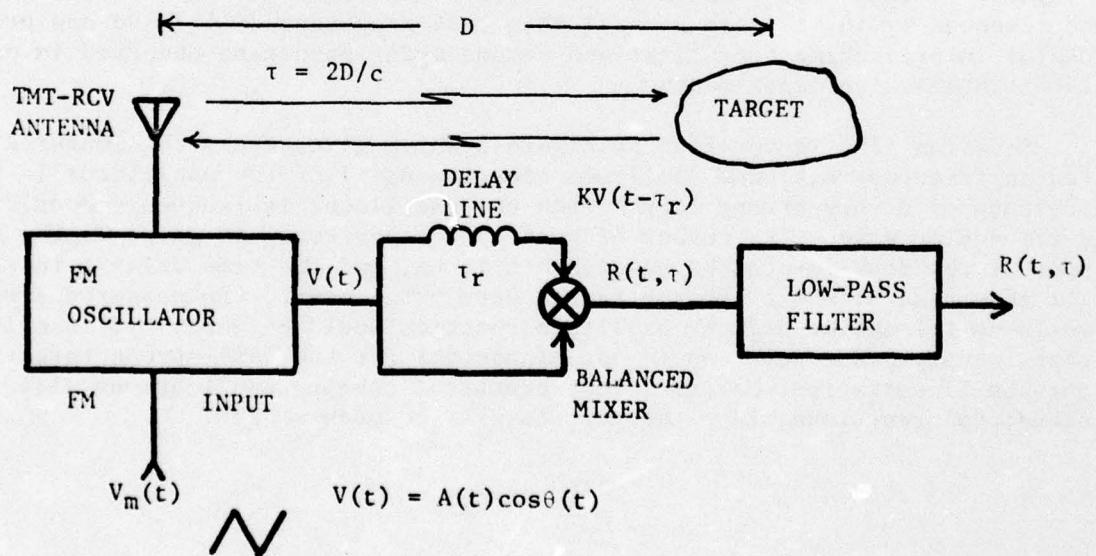


Figure 4. Frequency reaction correlator

Figure 4 illustrates the hardware implementation of the Frequency Reaction Correlator.

The delayed and undelayed oscillator voltages are applied to a balanced mixer. The undelayed mixer input is saturated so that amplitude variations at this input have no effect. The mixer output $R(t, \tau)$ is the product given by

$$R(t, \tau) = 2K_1 A(t - \tau_R) \cos \theta(t) \cos \theta(t - \tau_R) \quad (13)$$

where K_1 includes the attenuation of the RF delay line and the mixer conversion loss. Ignoring terms corresponding to the double frequency carrier, $R(t, \tau)$ becomes

$$R(t, \tau) = K_1 A(t - \tau_R) \cdot \cos [\theta(t) - \theta(t - \tau_R)] \quad (14)$$

The angular difference $\theta(t) - \theta(t - \tau_R)$ is given by

$$\psi(t) \triangleq \theta(t) - \theta(t - \tau_R) = \int_{t - \tau_R}^t \omega(t') dt' \approx \omega(t) \tau_R \quad (15)$$

where

$$\omega(t) = \omega_c(t) - \omega_s \sin [\omega_c(t) \tau] \quad .$$

Similarly, $K_1 A(t - \tau_R)$, by using (12) is

$$\begin{aligned} K_1 A(t - \tau_R) &= K_1 \{A_0 + a_s \cos [\omega_c(t - \tau_R) \tau]\} \\ &= A_R \left\{1 + \frac{A_s}{A_R} \cos [\omega_c(t) \tau]\right\} \quad . \end{aligned} \quad (16)$$

The approximation that $\dot{\omega}_c(t) \tau_R$ is small has been used in (16) and the substitutions $A_R = K_1 A_0$ and $A_s = K_1 a_s$ have been made. A_R , then, is the peak amplitude of the reference beat pattern out of the mixer with no signal present. Using (15) and (16) in (14), $R(t, \tau)$ then becomes

$$R(t, \tau) = \underbrace{A_R \left\{1 + \frac{A_s}{A_R} \cos [\omega_c(t) \tau]\right\}}_{\text{Envelope}} \cdot \underbrace{\{\cos [\omega_c(t) \tau_R - \omega_s \tau_R \sin (\omega_c(t) \tau)]\}}_{\text{Beat Waveform}} \quad (17)$$

Equation (17) describes the output time waveform from the balanced mixer as the oscillator radian frequency $\omega_c(t)$ is swept by the modulation voltage. In the absence of a target, we would expect the time waveform to be given by $A_R \cos[\omega_c(t) \tau_R]$, which is the beat between the delayed and undelayed RF voltages at the input to the mixer. When the target is present, because of the frequency reaction of the oscillator to the target signal, the beat is phase modulated as given by $\omega_s \tau_R \sin (\omega_c(t) \tau)$, and amplitude modulated by the target signal an amount A_s/A_R . The phase modulation is in synchronism with the expected phase of the beat when $\tau = \tau_R$ and causes stretching of one part of the beat cycle with respect to a part of the cycle differing in phase by 180° . The stretching and shrinking of the beat waveform will produce a positive average value when the positive half cycles are stretched. This change in average value corresponds with the doppler phase of the target. This effect

on the beat pattern is illustrated in Figure 5 for three target delays which are approximately equal to the reference delay but differ by 1/4 of a doppler cycle in delay time.

The amplitude reaction is small and is not discernable in the illustration. The effect of the phase modulation is evident in that $R(t, \tau_1)$ shows a beat pattern in which the frequency reaction caused by the target produces a positive average value, while for $R(t, \tau_3)$ it has a negative average value. The distortion due to frequency reaction is also evident in $R(t, \tau_2)$ but, for this value of τ , the average value is approximately zero. The variation in the average value of the mixer waveform $R(t, \tau)$ due to frequency and amplitude reaction of the oscillator is the correlator output. When the target is approaching the oscillator, these variations will occur at the doppler frequency and the doppler signal amplitude will peak up at a delay corresponding to that of the reference delay line.

The reaction response can be examined mathematically by assuming $\omega_s \tau_r$ is a small angle and expanding equation (17),

$$R(t, \tau) = A_r \left\{ 1 + \frac{A_s}{A_r} \cos[\omega_c(t)\tau] \right\} \cdot \left\{ \cos \omega_c(t)\tau_r + \omega_s \tau_r \sin[\omega_c(t)\tau] \sin[\omega_c(t)\tau_r] \right\} . \quad (18)$$

When the reaction is reasonably small, the second order term corresponding to $A_s/A_r \cdot \omega_s \tau_r$ can be dropped. $R(t, \tau)$ is then given approximately as the sum of three terms: the mixer beat pattern in the absence of target $R_b(t, \tau_r)$; a term $R_{am}(t, \tau)$ due to the amplitude reaction; and a term $R_{fm}(t, \tau)$ due to the frequency reaction. These terms are

$$R_b(t, \tau_r) = A_r \cdot \cos [\omega_c(t)\tau_r] \quad (19-1)$$

$$R_{am}(t, \tau) = A_r \cdot \frac{A_s}{A_r} \cos [\omega_c(t)\tau] \cdot \cos [\omega_c(t)\tau_r] , \quad (19-2)$$

and

$$R_{fm}(t, \tau) = A_r \cdot \omega_s \tau_r \cdot \sin [\omega_c(t)\tau] \sin [\omega_c(t)\tau_r] . \quad (19-3)$$

The first equation can be interpreted a reference beat pattern generated by the delay line, and the last two equations as a product of this reference beat with the signal beat generated by the target at delay .

When each of the terms in (19) are filtered by the low-pass filter following the mixer, the output of the filter will be the time average of each of the beats. This is recognized as correlation functions of the FM process given by

$$\overline{R_b(t, \tau_r)} = A_r \overline{\cos [\omega_c(t)\tau_r]} = A_r \cdot \rho(\tau_r)$$

$$\overline{R_{am}(t, \tau)} = A_r \cdot \frac{A_s}{A_r} \overline{\cos [\omega_c(t)\tau] \cos [\omega_c(t)\tau_r]} = \frac{A_r}{2} \cdot \frac{A_s}{A_r} \cdot [\rho(\tau - \tau_r) + \rho(\tau + \tau_r)]$$

$$\overline{R_{fm}(t, \tau)} = A_r (\omega_s \tau_r) \overline{\sin [\omega_c(t)\tau] \sin [\omega_c(t)\tau_r]} = \frac{A_r}{2} (\omega_s \tau_r) [\rho(\tau - \tau_r) - \rho(\tau + \tau_r)]$$

(20)

where $\rho(\tau)$ is the normalized autocorrelation of the frequency modulated carrier with no target present. $\overline{R_b(t, \tau_r)}$ is a DC term that does not contribute to the range response since it is not τ dependent. Equation (19-2) shows that the range response due to AM results from correlating an IF signal caused by amplitude reaction ($A_S/A_R \cos \omega_c(t)\tau$) with an IF reference ($A_R \cos \omega_c(t)\tau_r$). Correspondingly, the range response due to FM results from correlating an IF signal caused by frequency reaction ($\omega_s \tau_r \sin \omega_c(t)\tau$) with an IF reference ($A_R \sin \omega_c(t)\tau_r$). The delay line correlator simultaneously: (1) detects the IF signals due to amplitude and frequency reactions; (2) develops IF references corresponding to the reference delay; and (3) multiplies the IF signals by the reference to form an IF correlator.

The amplitude of $\overline{R_{am}(t, \tau)}$ can be compared to $\overline{R_{fm}(t, \tau)}$ by assuming the oscillator response is approximately that of a single tuned circuit and ω_s and a_s are related by

$$\omega_s = \frac{\omega_0 a_s}{2Q A_0} = \frac{\omega_t}{2} \cdot \frac{A_s}{A_r} \quad , \quad (21)$$

where ω_t is the oscillator tank bandwidth in radians/sec.

When the RF bandwidth B is such that $B\tau_r \gg 1$, the range response contributions due to terms proportional to $\rho(\tau + \tau_r)$ can be neglected for positive τ . The range response due to both amplitude and frequency reaction can then be simplified to

$$\overline{R_{am}(t, \tau_r)} + \overline{R_{fm}(t, \tau_r)} = \frac{A_r}{2} \cdot \frac{A_s}{A_r} \left[1 + \frac{\omega_t}{2} \tau_r \right] \rho(\tau - \tau_r) \quad . \quad (22)$$

For most ranging applications, the factor $\omega_t \tau_r / 2$ (which is the 'gain' of the FM with respect to AM) will exceed 1 and the range response due to AM can be neglected. The simplified range response is then given by

$$\overline{R_{fm}(t, \tau)} = \frac{A_s}{2} \left[\frac{\omega_t \tau_r}{2} \right] \rho(\tau - \tau_r) \quad ; \quad (23)$$

or, using (21),

$$\overline{R_{fm}(t, \tau)} = \frac{A_r}{2} \cdot \omega_s \tau_r \rho(\tau - \tau_r) \quad ,$$

where A_r is the peak value of the reference beat waveform at the output of the mixer.

As an example, when the RF power spectrum is uniform with bandwidth B and center frequency ω_0 , $\rho(\tau)$ is given by

$$\rho(\tau) = \frac{\sin \pi B \tau}{\pi B \tau} \cos \omega_0 \tau = \rho_0(\tau) \cos \omega_0 \tau \quad , \quad (24)$$

where $\rho_0(\tau)$ is the Fourier transform of the normalized baseband power spectrum. The FM term then provides the range response given by

$$\overline{R_{fm}(t, \tau)} = \frac{A_r}{2} (\omega_s \tau_r) \frac{\sin \pi B(\tau - \tau_r)}{\pi B(\tau - \tau_r)} \cos \omega_0(\tau - \tau_r) , \quad B\tau_r \gg 1 . \quad (25)$$

For testing and calibration purposes, the results for low modulation, or no modulation, are of interest. Here $B\tau_r \ll 1$. Then both $\rho_0(\tau - \tau_r)$ and $\rho_0(\tau + \tau_r)$ are approximately unity, and using (24), (20) becomes

$$\overline{R_{fm}(t, \tau)} = A_r (\omega_s \tau_r) \sin \omega_0 \tau \sin \omega_0 \tau_r , \quad B\tau_r \ll 1 . \quad (26)$$

This response for $B\tau_r \ll 1$ is a function of $\sin \omega_0 \tau_r$ and, when either ω_0 or τ_r is adjusted such that $\sin \omega_0 \tau_r$ is unity, the doppler amplitude is twice the amplitude at the $(\sin x)/x$ peak of the modulated response given by (25).

The measured range response for the example given in (25) is shown on Figure 6b together with an example of the unmodulated range response (Figure 6a, $B=0$) as given in (26). The range responses were measured using a shorted variable-length RF transmission line for the variable delay τ and exhibit an exponential attenuation factor as a multiplier of equations (25) and (26). In Figure 6d, the triangular modulation which produces the oscillator frequency variation from $f_0 - B/2$ to $f_0 + B/2$ is shown. In Figure 6c the IF beat pattern out of the mixer is displayed--as given by (17). That is, assuming negligible AM effect, $R(t, \tau) = A_r \cos(\omega(t)\tau_r)$, where $\omega(t)\tau_r$ is the sum of the phase of the beat pattern due to the modulation plus the pulling phase due to the target. A fixed target is evident in the beat pattern by the distortion of the cycles from a sine wave. The average value of the target distorted IF beat pattern, as the distance to the target (τ) is changed, is the range response Figure 6b. It has its maximum value at a target delay time, τ , corresponding to the delay line fixed delay, τ_r . The peak amplitude of this response should be one-half of the unmodulated response at the same target delay. As shown in Figure 6a, the unmodulated response is not quite twice that when modulated. This is because the discriminator operates about only one value of the beat pattern (marked with circles). If the beat pattern is not a perfect sinusoidal wave, then a difference from the factor of two would be expected.

Figure 7 shows the same series of recordings as that of Figure 6 but with the delay-line time delay, τ_r , increased by a factor of 2.25 times. The number of cycles in the beat pattern (Figure 7c) is increased by this factor and target time delay for the peak of the range response is also increased by the same factor. Somewhat surprising although predicted by the equations, is the fact that the peak amplitudes also increased by this factor of 2.25. This is because the delay line parameter, τ_r , appears as a factor in the amplitude of $\overline{R_{fm}(t, \tau)}$. Thus, for targets which have an amplitude attenuation proportional to $1/\tau$, the range response peak will be the same amplitude regardless of the value of the delay, τ_r , at which the peak occurs.

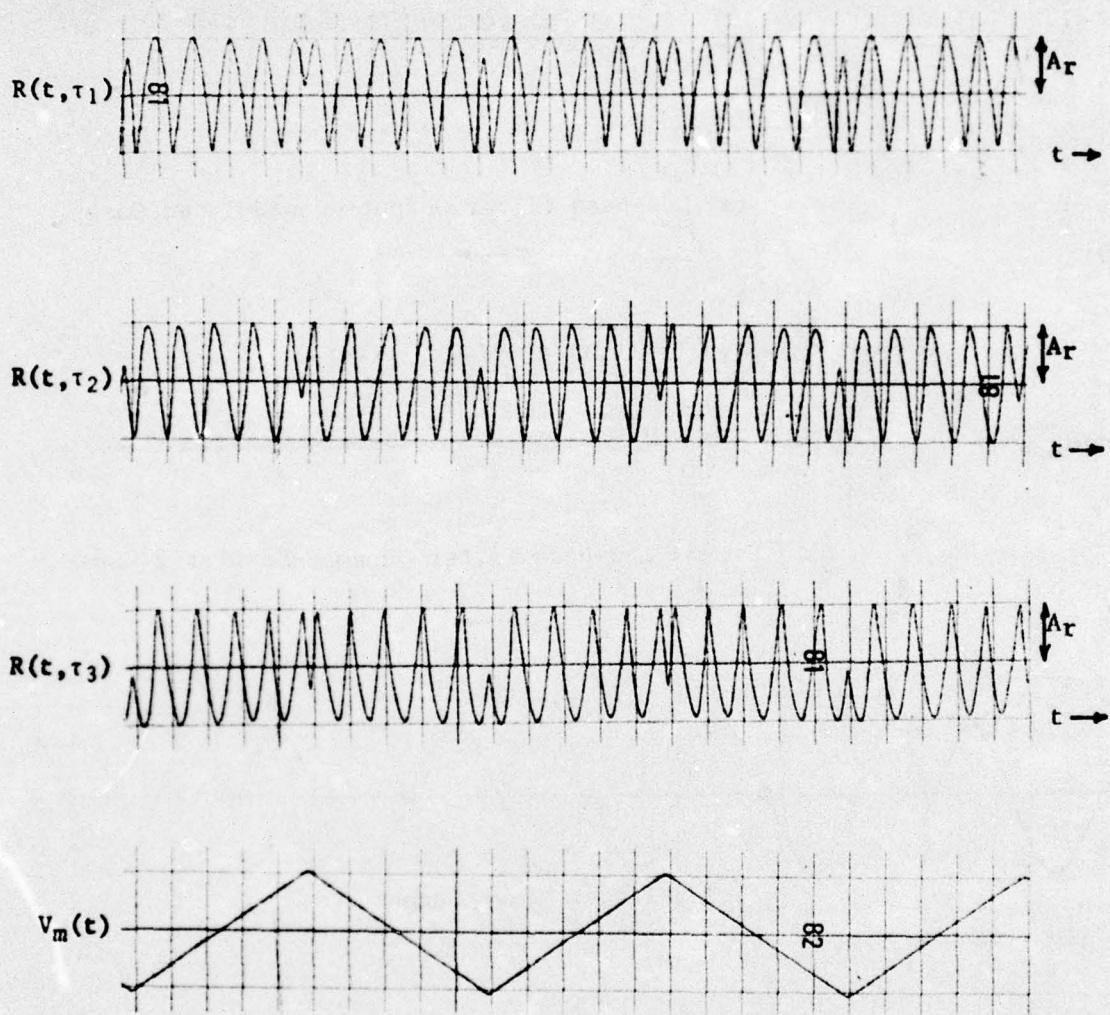


Figure 5. $R(t, \tau)$ for a very strong target signal when $\tau = \tau_r$. Triangle FM, $B\tau_r = 5$.

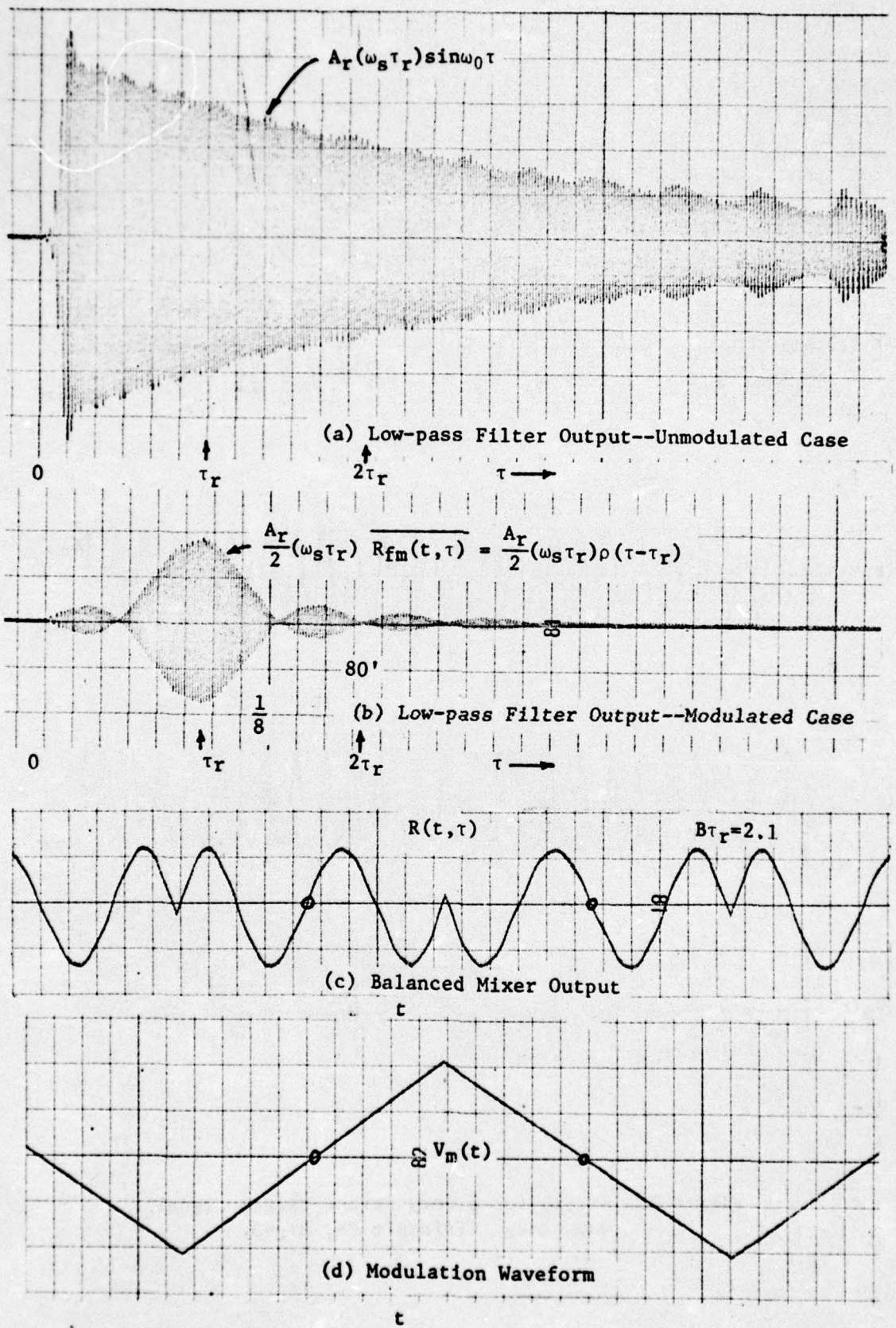


Figure 6. Waveforms for $\tau_r = 0.08 \mu\text{sec}$

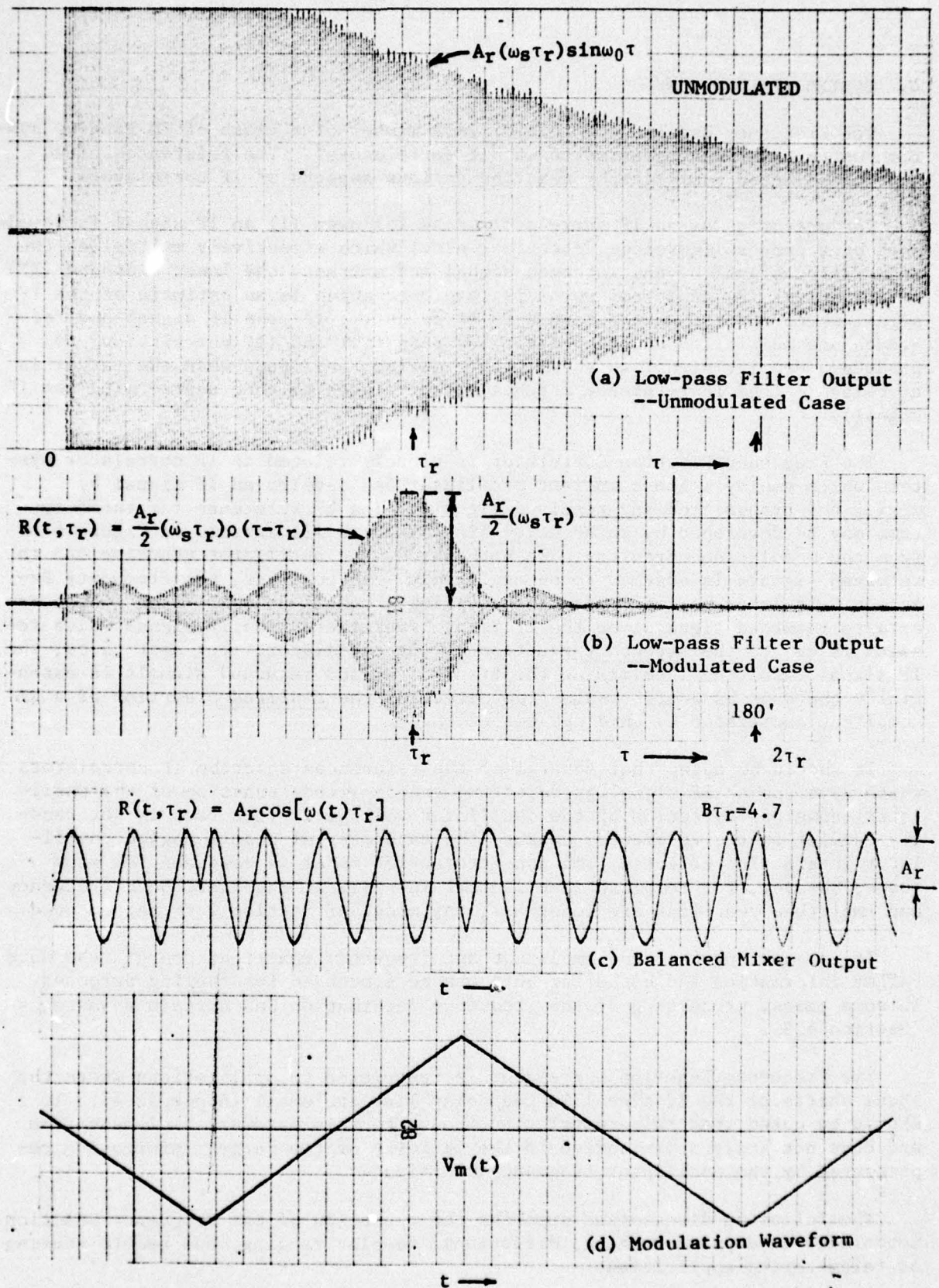


Figure 7. Waveforms for $\tau_r = 0.18 \mu\text{sec}$

4. SYSTEM APPLICATIONS

The Frequency Reaction Correlator is a member of a class of FM ranging systems which have been referred to as "IF correlators". The references cited and the selected bibliography describe various aspects of IF correlators.

The operation of an IF correlator is as follows: (1) an IF signal is developed by a process (envelope detection, etc.) which effectively multiplies the transmitted signal by the returned signal and extracts the lower sideband (IF) by filtering; (2) an IF reference is developed which is an estimate of the IF signal which results when a target is at delay τ_r ; (3) the IF signal and reference are multiplied and the result low pass filtered (IF correlation) to produce a doppler signal which will have maximum amplitude when the target is at delay τ_r (the IF reference matches or correlates to some degree with the IF signal).

The Frequency Reaction Correlator is closely related to IF correlator systems which employ a non-compliant oscillator and develop an IF signal by mixing the transmitted and received signals. The IF reference for these systems may be developed by an RF delay line/mixer as illustrated in Figure 4 or from the modulation circuitry. In both cases, the oscillator reaction due to returned signals is assumed to be negligible. In contrast, the Frequency Reaction Correlator is implemented by coupling a compliant oscillator (which reacts to returned signals) to the IF delay line/mixer. The IF signal which results is due to the frequency reaction of the oscillator. For most cases, the IF signal resulting from mixing the transmitted and returned signals is essentially the same as would result from detecting the amplitude reaction of a compliant oscillator by envelope detection.

It should be noted that several of the references describe IF correlators which develop an IF signal by detecting the amplitude reaction of the oscillator (envelope detection of the oscillator voltage). This fact is not readily evident in the references because the mathematical models neglect oscillator interaction effects. The non-interaction model is adequate for many cases; however, for compliant oscillators in applications where both frequency and amplitude reactions are important, the model of Section 2 is recommended.

It is apparent that the amplitude and frequency reactions contain the same target information and either or both can be processed for ranging purposes. In some cases, processing of the frequency information has certain advantages (Section 4.3).

The Frequency Reaction Correlator is restricted to applications where the phase shifts of the IF signal in the delay line are small (Appendix A). It should be noted that this restriction is due to this hardware implementation and does not imply a limitation in the validity of the target information represented by the oscillator frequency reaction.

The following discussions describe the operation of the Frequency Reaction Correlator in doppler ranging, directional doppler ranging, and remote sensing or telemetering applications.

4.1 Doppler Ranging

The Frequency Reaction Correlator can be implemented as previously illustrated in Figure 4 to obtain doppler range responses as indicated in Figures 6 and 7. Range responses which exhibit lower side-lobe levels can be obtained by controlling the transmitted power spectrum.³

4.2 Directional Doppler Ranging

By using two mixers in quadrature, the Frequency Reaction Correlator can be used to distinguish between approaching and receding targets (Figure 8).

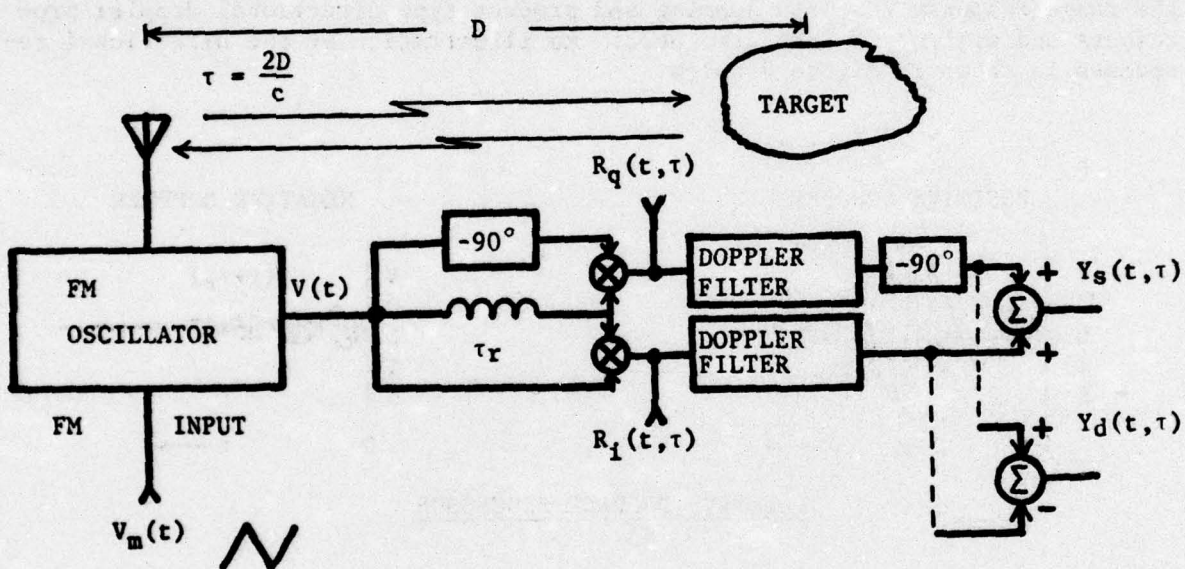


Figure 8. Directional doppler ranging

Using (18) and neglecting amplitude reaction effects, the in-phase mixer output can be written as

$$\begin{aligned}
 R_i(t, \tau) &= A_r \cdot \cos [\omega(t)\tau_r] \\
 &= A_r \{ \underbrace{\cos \omega_c(t)\tau_r}_{\text{Fixed Beat Pattern}} - \underbrace{\omega_s \tau_r \sin \omega_c(t)\tau_r}_{\text{Signal Beat Pattern}} \cdot \underbrace{\sin \omega_c(t)\tau_r}_{\text{Reference Beat Pattern}} \} \quad (27)
 \end{aligned}$$

³Bartlett, M.C. and Mattox, B.G., "Statistical Analysis of a Class of IF Correlator FM Ranging System," University of Florida Report for Harry Diamond Laboratories, Report No. HDL-CR-039-3, October 1974.

The quadrature channel can be written as

$$R_q(t, \tau) = A_r \cdot \sin [\omega_c(t) \tau_r]$$

$$= A_r \cdot \{ \underbrace{\sin \omega_c(t) \tau_r}_{\text{Fixed Beat Pattern}} + \underbrace{\omega_s \tau_r \sin [\omega_c(t) \tau]}_{\text{Signal Beat Pattern}} \cdot \underbrace{\cos [\omega_c(t) \tau_r]}_{\text{Reference Beat Pattern}} \} \quad (28)$$

These equations show that doppler signals are generated by correlating the IF signal, $\omega_s \tau_r \sin [\omega_c(t) \tau]$, with quadrature references $\sin[\omega_c(t) \tau_r]$ and $\cos[\omega_c(t) \tau_r]$. These doppler signals, when directionally processed, yield a range response proportional to $\rho(\tau - \tau_r)$ or $\rho(\tau + \tau_r)$ depending on whether the target is approaching or receding [4, Equation (41)]. Bartlett et al⁴ derived the range response for both summing and product type directional doppler processors and will not be repeated here. An illustration of the directional responses is shown in Figure 9 below

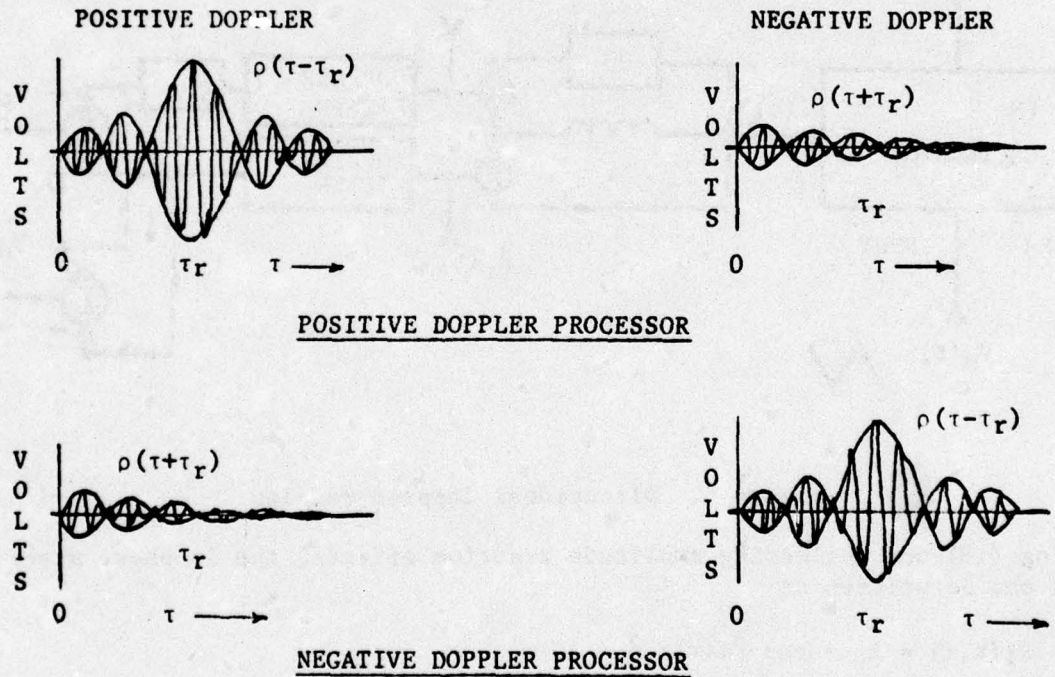


Figure 9. Directional doppler range responses

⁴Bartlett, M.C., Couch, L.W. and Johnson, R.C., "Directional Doppler Detection for IF-Correlator FM Ranging Systems Using General FM Modulations," University of Florida Report for Harry Diamond Laboratories, Report No. HDL-CR-039-5, October 1974.

This figure shows that, for approaching targets, the amplitude of the doppler voltage peaks-up out of the positive doppler processor; while for receding targets, the amplitude peaks-up out of the negative doppler processor.

Several measured examples of the output of a positive directional doppler processor are shown in Figures 10 through 13. Figures 10 and 11 show directional doppler range response for sawtooth and triangular FM modulation waveforms. These two modulations produce nearly identical range responses as given by a shifted $(\sin x)/x$ range law. Figure 12 shows the directional response for sine-wave FM. The range response is now given by a shifted $J_0(X)$ range law in agreement with the Fourier transform of the power spectrum. Figure 13 demonstrates that the directional doppler response is not affected if the FM modulation is itself frequency modulated by a lower frequency waveform. For this figure, a triangular wave is frequency modulated by a lower frequency triangular wave and the resulting waveform is used to frequency modulate an RF carrier. Since the probability density of the modulation, and thus the RF power spectrum, is still the same as for a triangle, the directional doppler response is the same as those of Figures 10 and 11.

4.3 Remote Sensing

In the previous section, it was shown that if a sample of the oscillator voltage is applied to a delay-line correlator, the pulling of the oscillator frequency by a target will produce an output voltage proportional to $\rho(\tau - \tau_r)$ of the RF waveform. Since the radiated RF waveform is also pulled, it may be received at a remote location and applied to a delay line correlator to produce the same $\rho(\tau - \tau_r)$ response as though the delay line correlator were connected to the oscillator. This remotely located receiver and delay-line correlator can then be made more complex so that targets at any time delay from the oscillator can be remotely sensed and tracked in range relative to the oscillator. Such a system is indicated in Figure 14.

In Figure 14 the output of the receiver can be used to drive the delay line, and range and range rate information are both unaltered. By using quadrature mixers at each delay-line tap, directional doppler information is also available from each output. Because only the frequency information of the receiver is used, the receiver can heterodyne the received signal to a convenient intermediate frequency and can employ hard limiting to improve the received S/N ratios. If the Q of the receiver band pass amplifier is greater than two, the output waveform will be sinusoidal even though limited in amplitude. This limiting is desirable in reducing AM effects such as signal fading and interference from other signals.

If the above system is used for surveillance, a number of oscillator sensors at different RF frequencies can be monitored by one receiving system if the receiving band is swept to each individual oscillator frequency by appropriately sweeping the local oscillator frequency.

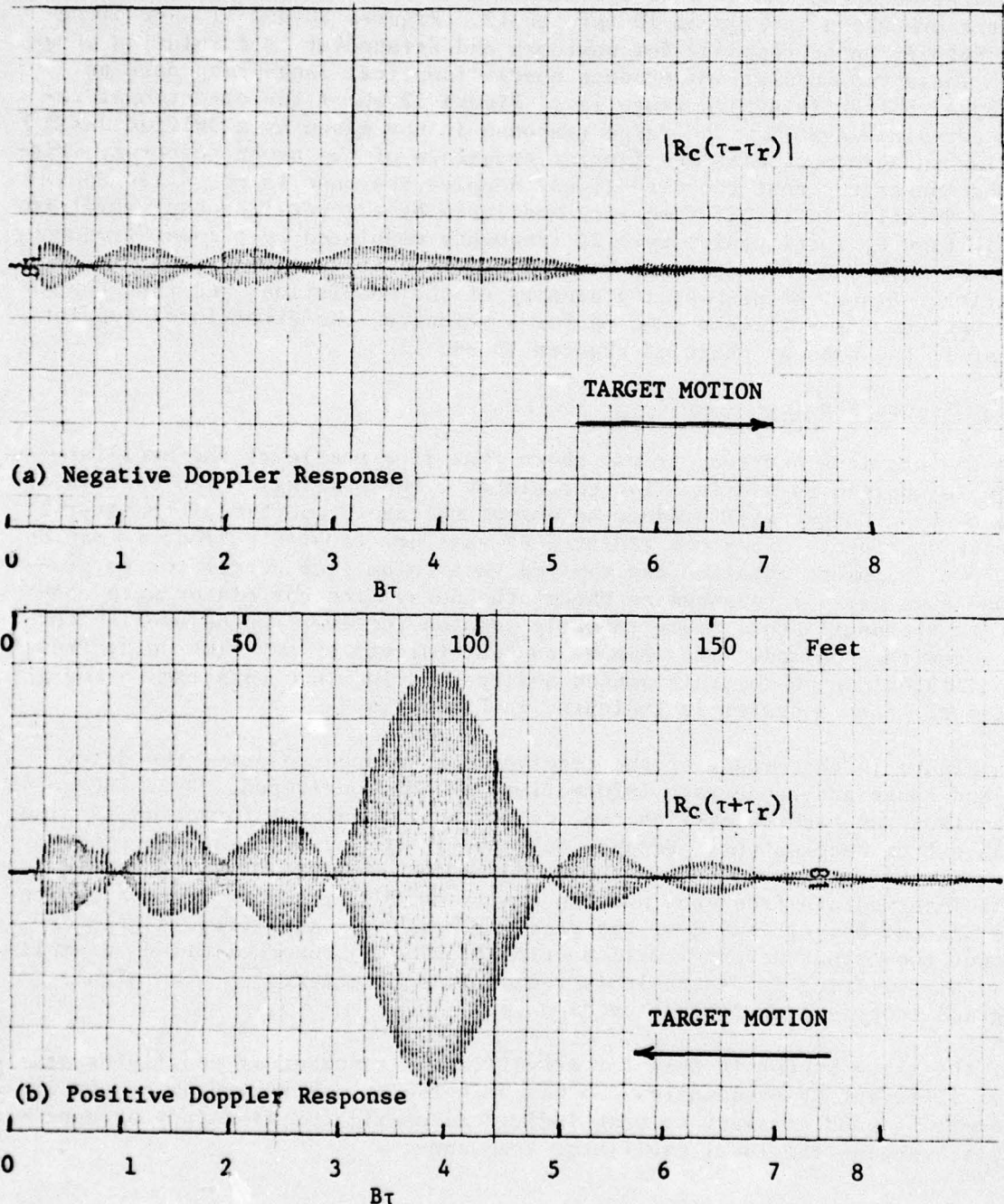


Figure 10. Directional doppler response for sawtooth FM

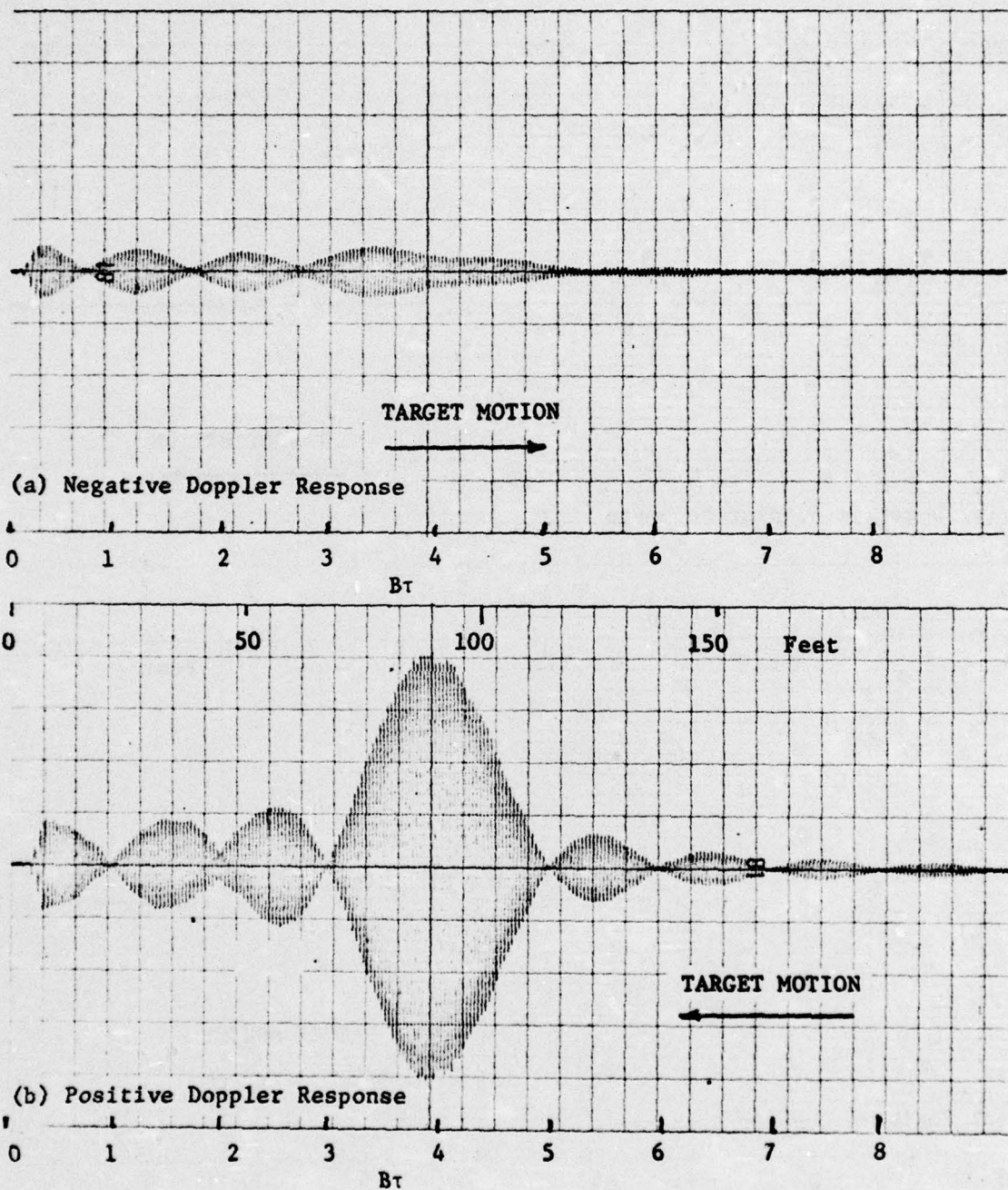


Figure 11. Directional doppler response for triangle FM

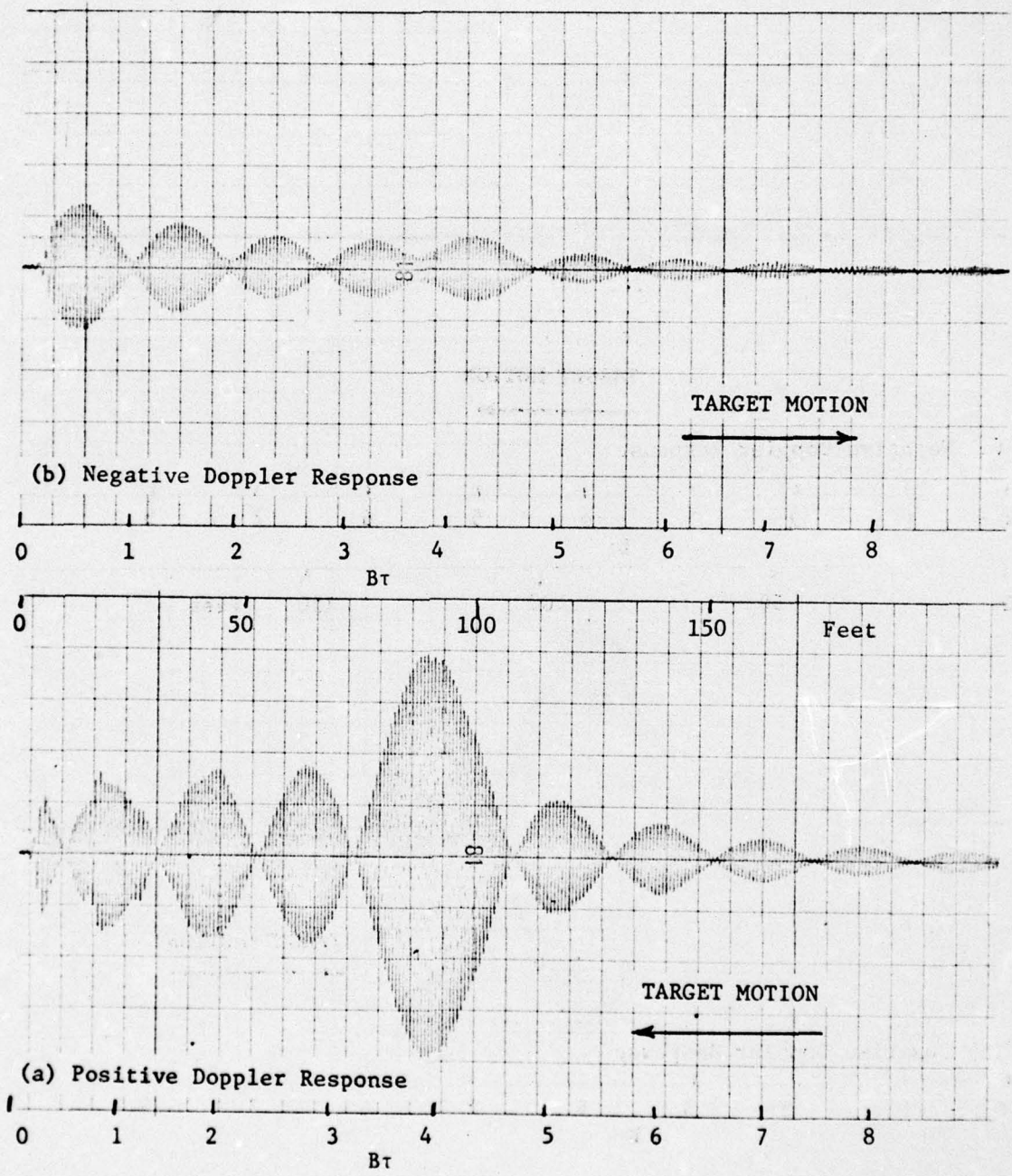


Figure 12. Directional doppler response for sine wave FM

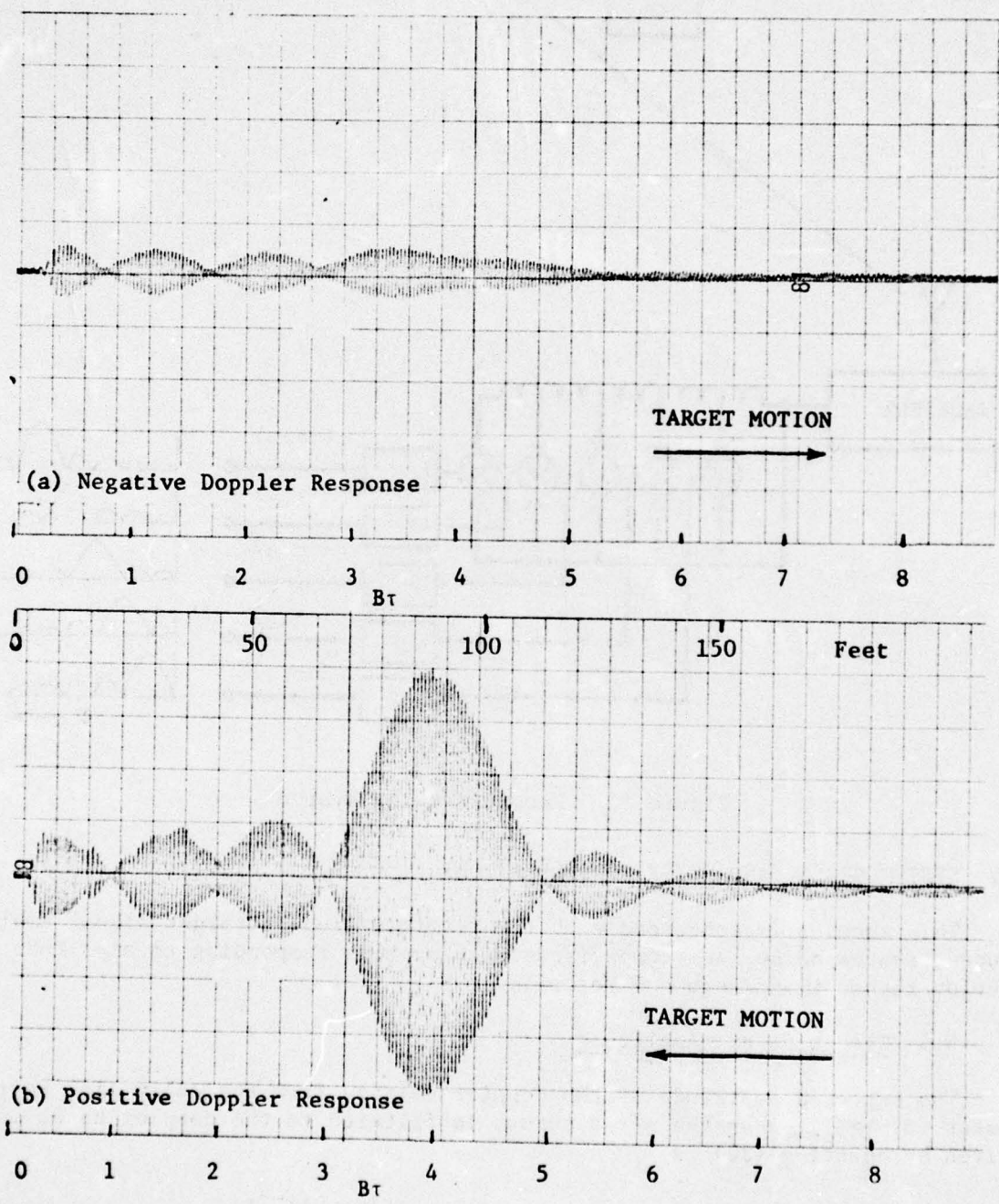


Figure 13. Directional doppler response for triangle/triangle FM/FM

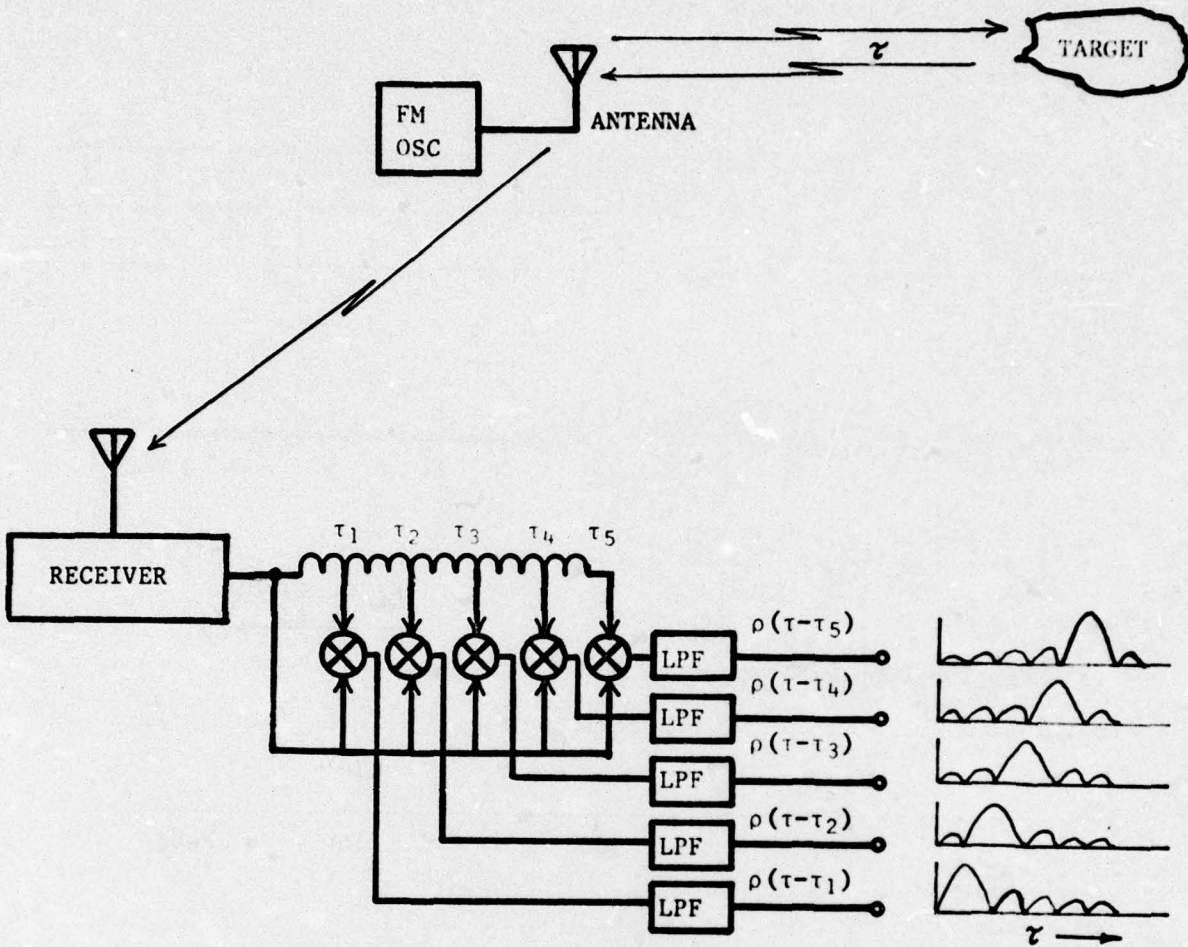


Figure 14. Remote ranging system

5. SYSTEM SIGNAL AND NOISE CONSIDERATIONS

This section is concerned with the determination of target signal amplitudes, system noise, and comparisons with systems responding to amplitude reaction rather than frequency reaction.

5.1 Target Signal Amplitude

The expected amplitude of the doppler voltage from the delay line correlator ($B\tau \gg 1$), when the mixer output is filtered to the doppler band, is given by equation (22) as

$$[VDOP]_{AM} + [VDOP]_{FM} = A_s \left[1 + \frac{\omega \tau \tau_r}{2} \right] \frac{\rho(\tau - \tau_r)}{2} \quad (29)$$

The detected doppler signals due to the AM and the FM reactions are in phase and fall in the doppler filter. The response due to the FM doppler is $\omega_t \tau_r / 2$ times that of the AM doppler. Examining this factor by substituting $2\pi c / \lambda Q$ for the radian frequency tank bandwidth, ω_t , and $2D_r / c$ for the reference delay time, τ_r , (29) becomes

$$[VDOP]_{AM} + [VDOP]_{FM} = A_s \left[1 + \frac{2\pi D_r}{Q\lambda} \right] \frac{\rho(\tau - \tau_2)}{2} \quad (30)$$

where D_r is the reference distance to the target.

Thus, for a reference delay line corresponding to a target at a reference distance, D_r , the FM response will exceed the AM response for $(D_r / \lambda) > (Q / 2\pi)$. The quantity $Q / 2\pi$ for an FM oscillator is usually about 10, so that the FM response will exceed the AM response for target distances greater than 10λ . This is usually the case and the effect of the AM response can then be ignored.

An interesting feature of (30) is that the doppler response from a target increases with distance D_r . Thus, if the target signal amplitude, A_s , decreases no faster than D^{-1} , the doppler response at the correlation peak, τ_r , will be constant and independent of the value of τ_r that is used in the system. This situation occurs for a ground-plane target where the signal amplitude A_s is given by $A_s = S_R (\Delta R / R_a)$. S_R is the voltage amplitude sensitivity factor of the oscillator to the radiation resistance R_a , and $\Delta R / R_a$ as a function of height, h , above a perfect infinite, ground-plane target is $\Delta R / R_a = 3\lambda / (8\pi h)$. S_R should be measured by a pole test in order to determine the signal amplitude A_s ; but, for a radiating oscillator where the radiation resistance is matched to the loss resistance, the value of S_R can be approximated by $S_R = \frac{1}{2} A_r$, where A_r is the amplitude of the reference beat waveform out of the delay line/mixer. Substituting these values in (30) and using only the FM response term, the doppler amplitude for a perfect ground plane target is given by

$$[VDOP]_{FM} = \frac{3A_r}{16Q} \left(\frac{h_r}{h} \right) \rho(\tau - \tau_r) \quad (31)$$

where $h_r = D_r$ for ground plane targets.

At the correlation peak $h = h_r$, the peak doppler response is independent of h . The peak amplitude of the doppler is then $20 \log 16Q/3$ dB below the reference amplitude, A_r . For a tank Q of 50, this doppler voltage is 49 dB below A_r regardless of the delay line lengths, τ_r , chosen for the correlation.

5.2 System Signal/Noise Ratios

If noise is present in the oscillator, the output of the delay line and mixer is given by

$$R(t, \tau_r) = [A_r + e_n(t)] \cos [\omega_c(t)\tau_r + \Delta\omega_n(t)\tau_r] \quad (32)$$

where it is assumed that one of the inputs to the balanced mixer in Figure 4, is saturated to eliminate the AM noise due to that input. Here, $e_n(t)$ is the AM noise from the oscillator and $\Delta\omega_n(t)$ is any FM noise present on the

oscillator. From (21) $\Delta\omega_n(t)$ is related to $e_n(t)$ by

$$\Delta\omega_n(t) = \frac{\omega_t}{2A_r} e_n(t) \quad (33)$$

By expanding (32) we can determine the main contributing factors for the noise cross-products to be

$$n_{AM}(t) = e_n(t) \cos [\omega_c(t)\tau_r] \quad (34)$$

$$n_{FM}(t) = e_n(t) \left[\frac{\omega_t \tau_r}{2} \right] \sin [\omega_c(t)\tau_r] .$$

When these two cross-products are averaged in the doppler bandwidth, they produce a noise contribution according to that part of the convolution of the noise spectrum and reference beat spectrum which falls in the doppler bandwidth. If the noise term $e_n(t)$ is assumed to be of narrow bandwidth, b_n , then the noise spectrum is the convolution shown below for triangular FM.

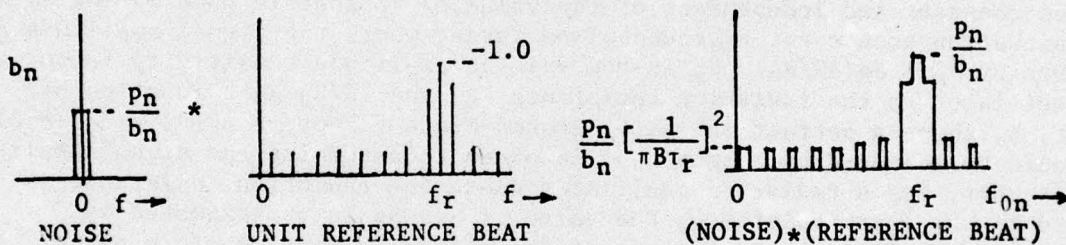


Figure 15. Power spectrum of $e_n(t)\cos[\omega_c(t)\tau_r]$ for narrow band $e_n(t)$ centered on zero

The total noise power, p_n , is the mean square value of the noise. The noise power, P_N , picked up in the doppler bandwidth, b_d , is then given by

$$[P_N]_{AM} = \overline{e_n^2} \left(\frac{b_d}{b_n} \right) \left[\frac{1}{\pi B \tau_r} \right]^2 \quad (35)$$

$$[P_N]_{FM} = \overline{e_n^2} \left(\frac{b_d}{b_n} \right) \left[\frac{1}{\pi B \tau_r} \right]^2 \left[\frac{\omega_t \tau_r}{2} \right]^2 .$$

The total noise due to both AM and FM is then

$$[P_N]_{TOTAL} = \overline{e_n^2} \left(\frac{b_d}{b_n} \right) \left[\frac{1}{\pi B \tau_r} \right]^2 \left[1 + \left(\frac{\omega_t \tau_r}{2} \right)^2 \right] . \quad (36)$$

The doppler signal power is obtained from (23).

$$P_S = \frac{A_s^2}{8} \left[\frac{\omega_t \tau_r}{2} \right]^2 \quad (37)$$

so that the resulting signal-to-noise in the doppler band is given by the ratio

$$\frac{P_S}{P_N} = \left[\frac{A_S^2}{2} \frac{1}{e_n^2} \right] \left(\frac{b_n}{b_d} \right) \left[\frac{\pi B \tau_r}{2} \right]^2 \frac{\left[\frac{\omega \tau_r}{2} \right]^2}{1 + \left[\frac{\omega \tau_r}{2} \right]^2} \quad (38)$$

The first bracketed term of (38) is the signal-to-noise ratio expected from an envelope detector and the remaining terms provide an increase in P_S/P_N as $B\tau_r$ is increased. This is an interesting result because it shows that for low-frequency noise, the signal-to-noise improves as either the RF bandwidth, B , or the delay line length, τ_r , is increased. This is no different, of course, than would be expected of any IF system having a $[\sin(x)]/x$ shaped IF passband and a center frequency corresponding to the expected signal frequency of a target at delay τ_r .

In summary, it was shown that for a perfect ground plane target the expected signal from the delay line correlator is a constant having a value of about 50 dB below the reference beat amplitude. Allowing for 20 dB of target signal deterioration because of poor reflection, then, in order for the noise to be less than the minimum doppler signal, the noise after filtering in the doppler band must be no greater than 70 dB below the reference beat amplitude. AM noise modulation of the oscillator is attenuated the most, and FM noise of the oscillator at low frequencies is also attenuated. However, any FM noise of the oscillator at the IF frequency is unattenuated and should be avoided, where possible, by low-pass filtering of the modulation waveform.

6. SYSTEM IMPLEMENTATION CONSIDERATIONS

6.1 Functional Requirements

The Frequency Reaction Correlator estimates range by doppler filtering a beat pattern which can be written as $\cos \theta = \cos[\omega(t)\tau_r + \theta]$, where τ_r and θ are constants. It is important to note that θ varies only with the oscillator radian frequency ω rather than its instantaneous phase. This fact allows the use of simplified digital processing techniques for measuring the angle θ (Section 6.3). Also, the function $\cos \theta$ can be generated by various methods provided θ is properly measured. Since τ_r is a constant, θ is seen to be directly proportional to oscillator frequency; therefore, a measurement of oscillator frequency provides the necessary information. While the system has been explained in the previous discussions using RF delay line/mixer hardware, any implementations which synthesizes the beat pattern will produce the required results. For example, a discriminator might be used to produce a voltage proportional to oscillator frequency $\omega(t)$ and the beat pattern $\cos[\omega(t)\tau_r + \theta]$ accomplished by function generator techniques.

The sensitivity of the ranging system is an important factor in considering hardware techniques. For ranging on weak targets, the doppler signal may be more than 70 dB below the mixer beat pattern. For this reason, self noise is an important factor in determining hardware techniques for implementing the Frequency Reaction Correlator.

6.2 RF Delay Line/Mixer Implementation

The RF delay line/mixer is a straight-forward implementation of the Frequency Reaction Correlator and may be preferred for applications where cost and weight are not overriding considerations. This implementation uses passive hardware techniques and thus does not introduce additional noise; however, there are disadvantages which must also be considered. The oscillator will exhibit noise-like fluctuations of both amplitude and frequency which could limit the system performance. Ideally, if both delayed and undelayed mixer inputs are saturated, the oscillator amplitude variations will have no effect. In practice, an output due to mixer unbalance (typically attenuated by 40 dB) will be generated which varies with oscillator amplitude. By this means, the oscillator amplitude noise variations are coupled to the doppler amplifier. The unbalance effect can also be caused by leakage across the delay line. This is usually not a problem for transmission-line type delay lines but was found to be a serious problem in some experimental crystal acoustic delay lines. Experiments indicated that the Frequency Reaction Correlator could be satisfactorily implemented with RF delay line/mixer approach provided high quality delay lines and mixers are available. This implementation may be desirable for applications such as remote sensing where cost and weight are not overriding considerations.

6.3 Digital Delay Line/Mixer Implementation

6.3.1 Operating Principles

The RF delay line/mixer hardware available during the course of this study was not considered suitable for low-cost, light-weight ranging applications; consequently, alternative hardware implementation techniques were investigated. The most promising technique investigated consists of mixing the FM oscillator signal with a local oscillator (L.O.) to obtain an intermediate frequency signal whose axis crossings are processed digitally to obtain the required beat pattern. This system is illustrated in Figure 16.

The oscillator signal with center frequency ω_0 is mixed with the local oscillator (L.O.) at $\omega_{LO} = \omega_0 \pm \omega_1$ to produce a difference frequency at ω_1 . The local oscillator frequency is set so that the bandwidth to center frequency ratio ($2\pi B/\omega_1$) at point A is approximately unity, whereas, the RF bandwidth to center frequency ratio ($2\pi B/\omega_0$) is typically 1/20 or less. This ratio is important in determining the number of discrete elements required for the delay mechanism. The low level signal at A is converted to TTL logic levels using an ECL/TTL level converter. The system was tested with an RF bandwidth of 20 MHz. The L.O. was adjusted to give a band at A from 10 to 30 MHz. The ECL/TTL output waveform varies with frequency and is quite asymmetrical at the upper frequency range. The ± 2 FF is used to restore the symmetry of the waveshape at the expense of reducing the bandwidth by 2; consequently, a digital delay of $2\tau_r$ is required to produce a range response which peaks at $\tau_r(B\tau_r = B/2 (2\tau_r))$.

The output of C drives a series chain of TTL inverters which have a propagation delay of about 6 ns each. The product of the delayed and undelayed signals is obtained digitally by an exclusive OR gate whose output is

lowpass filtered to obtain the desired beat pattern. The experimental system used 108 gates to achieve a delay of ≈ 650 ns. Since the effective delay is 325 ns, the $B\tau_r$ product is then ≈ 6.5 . The beat pattern for ranging is obtained from point E.

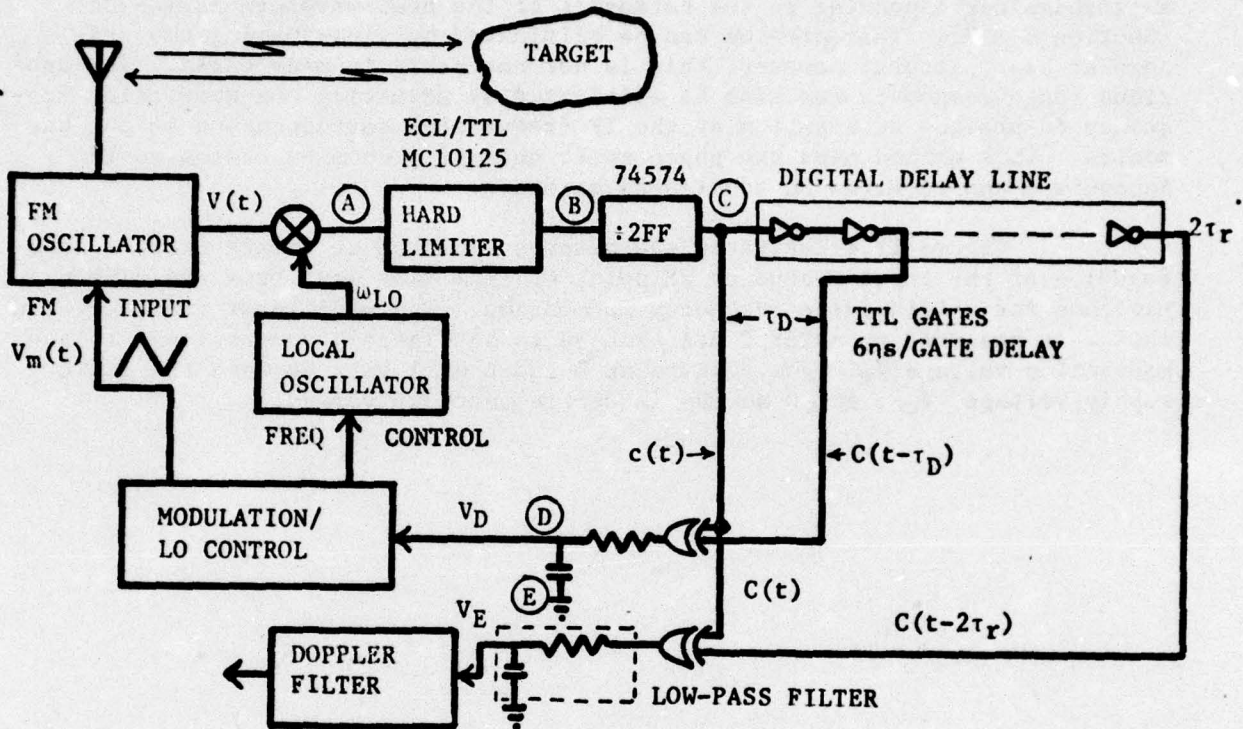


Figure 16. Digital delay line/mixer system

Control of the FM oscillator/L.O. frequencies are necessary to insure that the band at A falls within the frequency range of the digital hardware. To provide this control a linear frequency discriminator is implemented by using a short delay tap τ_D and an additional logic gate. In addition to controlling the band center frequency, the control loop bandwidth can be set to minimize low frequency FM oscillator frequency fluctuations which may arise; that is, the oscillator frequency variations can be attenuated for disturbances below the IF signal frequency, ω_r , providing the same effect as a high-pass IF filter.

By properly choosing the modulation frequency, the phase shift phenomena (Appendix A) can be used to attenuate the range response beyond the desired delay time. This acts somewhat like a low-pass IF filter, which, when combined with the high-pass filtering of the control loop, provides an IF band-pass filter. The IF filtering effect is important because filtering cannot be achieved directly because the IF signal is not explicitly generated in the Frequency Reaction Correlator.

Since the delayed and undelayed signals are square waves, the beat pattern at D and E will be triangular rather than sinusoidal. For the control loop frequency discriminator (D) this is desirable since a portion of a triangle gives a linear frequency discriminator characteristic. The triangular beat pattern at E can produce spurious range response at time delays and amplitudes corresponding to the harmonics of the beat waveform harmonics (Section 6.3.2). This problem can be eliminated by sine-shaping the triangular beat pattern; however, this is not necessary in many cases. The spurious range responses can also be eliminated by adjusting the modulation frequency to provide attenuation at the IF frequencies corresponding to the harmonics. This method uses the phase shift cut-off phenomena discussed in Appendix A and requires no additional hardware.

Figure 17 illustrates the outputs expected at points D and E as a function of the input frequency at point C. The time waveforms are also sketched for a triangular frequency modulation. The oscillator frequency and thus ω as measured at point C are assumed to be linearly proportional to the modulation voltage V_m . The outputs at D and E will vary between the logic supply voltage, V_{cc} , and 0 as the input frequency is varied.

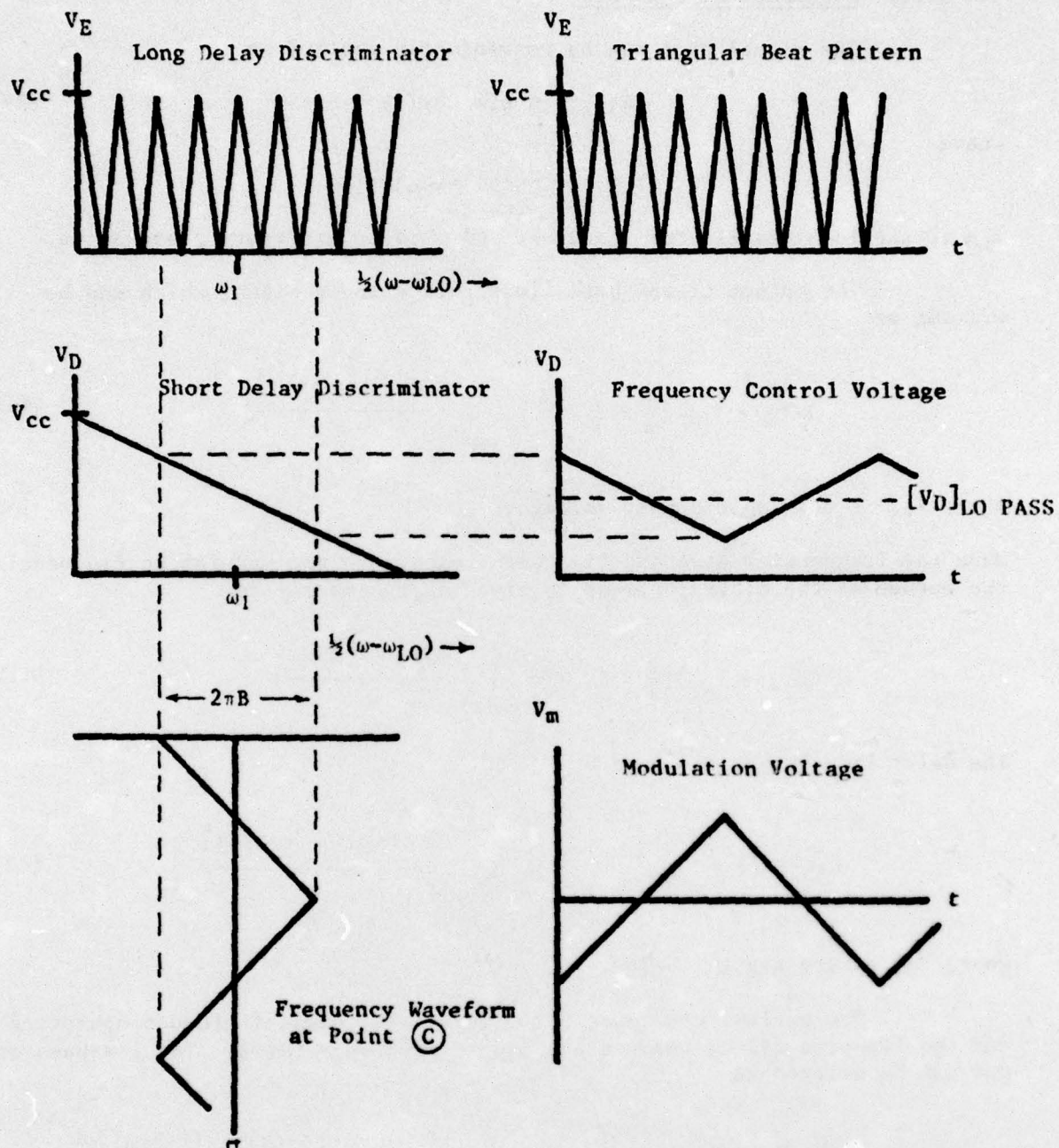


Figure 17. Theoretical digital delay line/mixer waveforms

6.3.2 Mathematical Analysis

The signal at A can be conveniently written as

$$A(t) = K \sin 2\theta_1(t) \quad (39)$$

where

$$2\theta_1(t) = \int_0^t [\omega(t') - \omega_{LO}] dt' + \phi$$

ω_{LO} is the local oscillator frequency and ϕ is an arbitrary phase angle.

The output of the hard limiter is a logic signal which can be written as

$$B(t) = V_{CC} \left[\frac{1}{2} + \frac{1}{2} \cdot \frac{4}{\pi} \sum_{n \text{ odd}} \frac{\sin[n \cdot 2\theta_1(t)]}{n} \right] \quad (40)$$

where V_{CC} is the logic supply voltage.

When the frequencies at A are high with respect to the modulation frequencies, the output of the binary divider is given approximately as

$$C(t) = V_{CC} \left[\frac{1}{2} + \frac{1}{2} \cdot \frac{4}{\pi} \sum_{n \text{ odd}} \frac{\sin[n \cdot \theta_1(t)]}{n} \right] \quad (41)$$

The delay line output is given by

$$C(t-2\tau_r) = V_{CC} \left[\frac{1}{2} + \frac{1}{2} \cdot \frac{4}{\pi} \sum_{n \text{ odd}} \frac{\sin[n \cdot \theta_1(t-2\tau_r)]}{n} \right] \quad (42)$$

where $2\tau_r$ is the digital delay.

The exclusive-OR gate performs a 1-bit digital product operation and the low-pass filter removes the double-frequency terms. The low-pass output can be written as

$$V_E(t) = \frac{2C(t)C(t-2\tau_r)}{2} = V_{CC} \left[\frac{1}{2} + \frac{1}{2} \frac{8}{\pi^2} \sum_{n \text{ odd}} \frac{\cos n[\theta_1(t) - \theta_1(t-2\tau_r)]}{n^2} \right] \quad (43)$$

where a gain of 2 is needed so that the peak-to-peak output is V_{CC} .

The angle can be expanded as

$$\begin{aligned} \theta_1(t) - \theta_1(t - 2\tau_r) &= \frac{1}{2} \left[\int_0^t \omega(t') dt' - \omega_{LO}t + \phi - \int_0^{t-2\tau_r} \omega(t') dt' + \omega_{LO}t - \omega_{LO}2\tau_r - \phi \right] \\ &= \frac{1}{2} \left[\int_{t-2\tau_r}^t \omega(t') dt' - \omega_{LO}2\tau_r \right]. \end{aligned} \quad (44)$$

Using the approximation of Appendix A, (43) simplifies to

$$V_E(t) = V_{CC} \left[\frac{1}{2} + \frac{1}{2} \cdot \frac{8}{\pi^2} \sum_{n \text{ odd}} \frac{\cos \frac{n}{2} [\omega(t)2\tau_r - \omega_{LO}2\tau_r]}{n^2} \right] \quad (45)$$

$$= V_{CC} \left[\frac{1}{2} + \frac{1}{2} \cdot \frac{8}{\pi^2} \sum_{n \text{ odd}} \frac{\cos n [\omega(t)\tau_r - \omega_{LO}\tau_r]}{n^2} \right] \quad (46)$$

Equation (46) describes a triangular beat pattern with an arbitrary phase shift $\omega_{LO}\tau_r$ introduced by the local oscillator. The first harmonic is the term required for the Frequency Reaction Correlator. Note that the low-pass filter in Figure 17 is not required for system operation. That is, it is needed only so that the beat pattern can be observed.

The logic signal from the exclusive-OR gate can be converted to any desired voltage amplitude before filtering to obtain "gain" if desired. For most applications, gain is not needed since the first harmonic amplitude is $V_{CC} \cdot 4/\pi^2$.

To examine the manner in which the beat pattern harmonics cause spurious range responses, the oscillator frequency as given by (12), $\omega(t) = \omega_c(t) - \omega_s \sin [\omega_c(t)\tau]$, is substituted into (46) to give

$$V_E(t) = V_{CC} \left[\frac{1}{2} + \frac{4}{\pi^2} \sum_{n \text{ odd}} \frac{\cos n [\omega_c(t)\tau_r - \omega_{LO}\tau_r - \omega_s\tau_r \sin (\omega_c(t)\tau)]}{n^2} \right]. \quad (47)$$

Expanding using small angle approximations, we have

$$\begin{aligned} V_E(t) &= V_{CC} \left[\frac{1}{2} + \frac{4}{\pi^2} \sum_{n \text{ odd}} \frac{\cos n [\omega_c(t)\tau_r - \omega_{LO}\tau_r]}{n^2} \right. \\ &\quad \left. + \omega_s\tau_r \sin \omega_c(t)\tau \sum_{n \text{ odd}} \frac{1}{n} \sin n [\omega_c(t)\tau_r - \omega_{LO}\tau_r] \right]. \end{aligned} \quad (48)$$

Equation (48) describes the triangular beat pattern corresponding to the reference delay along with the product of the signal beat and a series of harmonic references. By writing the references as $\sin[\omega_c(t) \cdot n\tau_r - \omega_{LO}n\tau_r]$, it is evident that since harmonic references corresponding to delays $\tau = n\tau_r$ are generated, the range responses will have components corresponding to these time delays. This means that the harmonic range responses neglecting space losses, are proportional to $1/n$. The harmonic range responses are unacceptable for many applications and can be eliminated or reduced by the methods discussed previously.

6.3.3 Test Results

Figures 18a and 18b illustrate the digital delay line correlator waveforms at points D and E for triangular modulation. The RF bandwidth was 20 MHz. The short delay line (V_D) used for a discriminator is operated with $B\tau_0 \approx 1/6$. This value gives a linear frequency discriminator and allows a reasonable L.O. frequency drift without producing ambiguities. This output can be used to control the average and low frequency difference between the FM oscillator and the L.O. as discussed in the previous section.

The ranging system output (V_E) exhibits the triangular beat pattern with $B\tau_r \approx 6.5$. The exact starting phase of the beat pattern depends on $\omega_{LO}\tau_r$ as indicated by the mathematical analysis. The measured range response for this system is illustrated in Figure 18c for a 10 KHz modulation frequency. This modulation frequency results in attenuation of the harmonic range response due to the phase shift discussed in Appendix A.

The attenuation of the harmonic range responses could not be verified for the conditions of Figure 18 due to limitations of the test apparatus.

To exhibit the attenuation, Figure 19 illustrates the range response for $B\tau_r \approx 2$ where the 3rd harmonic response can be observed. For the first case (19a), the modulation frequency was 1 KHz and the 3rd harmonic response is readily apparent. For the next case (19b), the modulation frequency is increased to 100 KHz and, consequently, the 3rd harmonic response is attenuated due to the phase shift.

The digital delay line showed a 1% variation in delay per 2% variation in logic supply voltage. The delay technique illustrated performed very well experimentally and is a simple and economical method of implementing the Frequency Reaction Correlator.

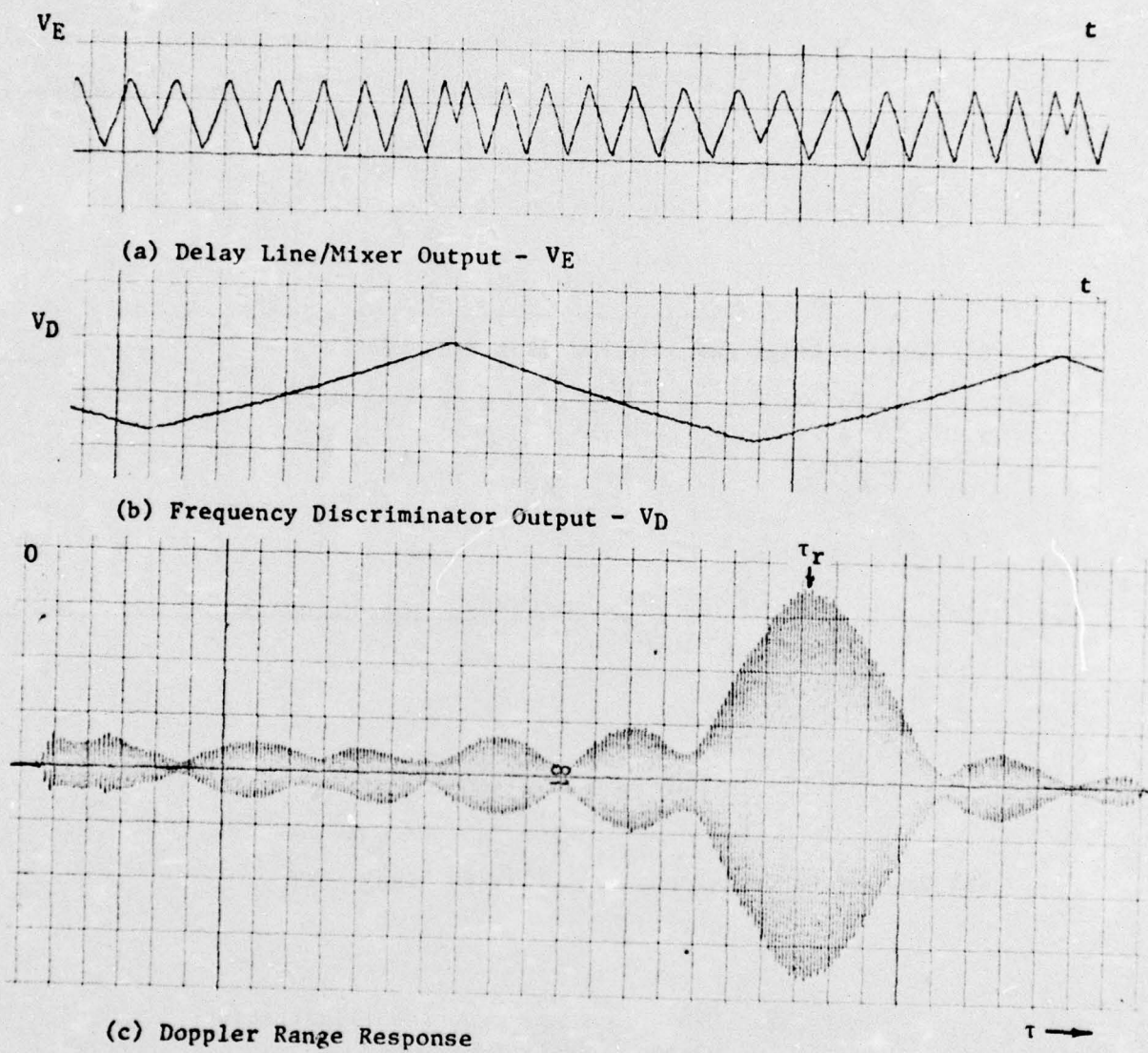
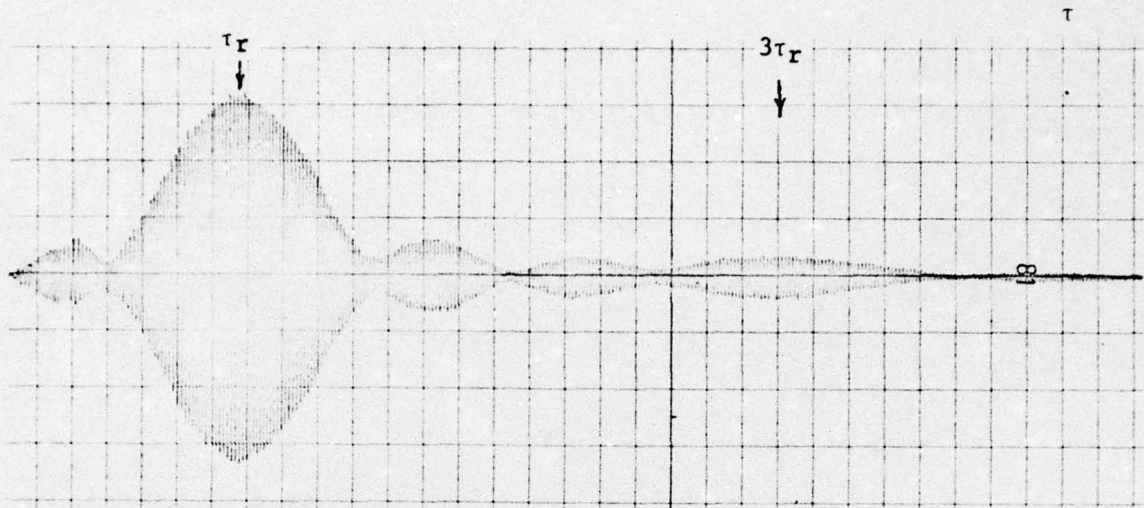
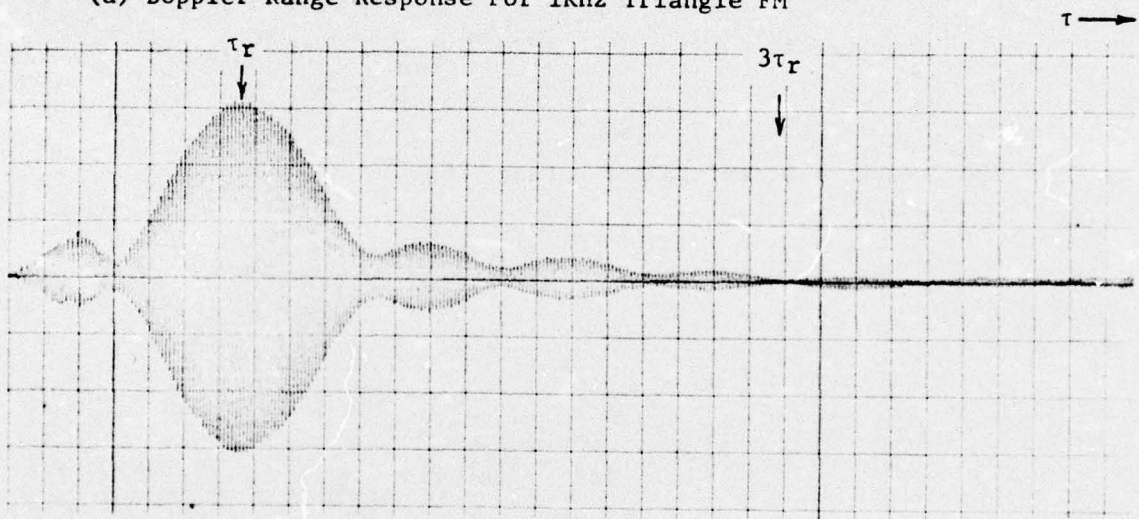


Figure 18. Measured responses for digital delay line/mixer
 $B\tau_r \approx 6.5$, $B=20$ MHz, $f_m=10$ KHz, triangular modulation



(a) Doppler Range Response For 1KHz Triangle FM



(b) Doppler Range Response For 100KHz Triangle FM

Figure 19. Measured range response illustrating harmonic range responses

7. CONCLUSIONS

A new type of distance measuring system which measures target range by detecting the frequency reaction of a target signal on the frequency of a frequency modulated oscillator was demonstrated to perform according to theoretical analyses. It was shown that a simple delay-line discriminator can be used to extract the target information from the oscillator RF voltage and that after filtering in the doppler band, the range response peaks at the delay-line time delay according to the shifted autocorrelation of the transmitted RF voltage. Using the same delay line and a second mixer, quadrature doppler signals were developed to implement a directional doppler response from the target.

For applications where an RF delay line cannot be used, it was demonstrated that a digital delay line employing the delay of TTL inverters provides satisfactory ranging.

A unique feature of frequency reaction is that the target information is carried on the transmitted waveform. Because of this, a remotely located receiving station can process the RF waveform of a frequency modulated sensor by means of a delay-line correlator. Both range and range-rate information of a target signal with respect to the sensor is then available at the remote station. This offers the advantage that the sensor is required only to transmit a frequency modulated carrier while all of the signal processing can be done remotely and with greater sophistication than could be obtained in the small space of the sensor.

SELECTED BIBLIOGRAPHY

Bartlett, M.C., "Harmonic Triangular FM Doppler Fuzing Systems For Low Height Applications," University of Florida Report No. 0164-1, February 1, 1973, AD No. 524-324. (SECRET)

Cross, J.L., "Effect of Amplitude Modulation on FM Ranging Systems," University of Florida Report No. 0058-5, November 17, 1971, AD No. 520-081. (CONFIDENTIAL)

Couch, L.W., "Range Laws For Distance Measuring Systems Using Frequency Modulation With a Nonlinear Triangular Waveshape," University of Florida Report No. 0058-8, March 28, 1972, AD No. 744-483.

Couch, L.W., and Johnson, R.C., "Range Laws For FM Radars With Harmonic Processing and Arbitrary Modulating Waveshapes," University of Florida Report No. 0169-1, November 14, 1973, AD No. 773-713/3GA.

Tozzi, L.M., "An FM Fuze System Using Synchronous Detection," Harry Diamond Laboratories Report No. TR-415, December 6, 1956. (CONFIDENTIAL)

Tozzi, L.M., "Resolution in Frequency-Modulated Radars," Ph.D. Dissertation, University of Maryland, 1972.

Mattox, B.G., "Improvement of the Range Response of Short Range FM Radars," Ph.D. Dissertation, University of Florida, 1975.

APPENDIX A

ATTENUATION FACTOR CAUSED BY PHASE SHIFT
OF THE OSCILLATOR REACTION BY THE DELAY LINE

It will be shown herein that the range response of the delay line correlator contains a factor which can produce attenuation of the expected target signal. The attenuation occurs when the product of the target beat frequency and the time-delay of the delay line is not small. This product represents a phase shift of the frequency reaction with respect to the reference beat waveform generated at the output of the delay line/mixer. The result of this phase shift is to produce a $\sin \xi/\xi$ type of range cut-off which may be useful, in some cases, in improving the range response of the system; whereas, in other cases, it may place a limitation on the maximum range of the system.

The system to be analyzed is as shown on Figure A-1. The input to the delay line is the constant amplitude RF waveform $\cos[\theta(t)]$ and the output of the balanced mixers $\cos[\psi(t)]$, where, using (15)

$$\psi(t) = \theta(t) - \theta(t - \tau_R) = \int_{t - \tau_R}^t \omega_C(t') dt' - \omega_S \int_{t - \tau_R}^t \sin[\tau \omega_C(t')] dt' \quad (A-1)$$

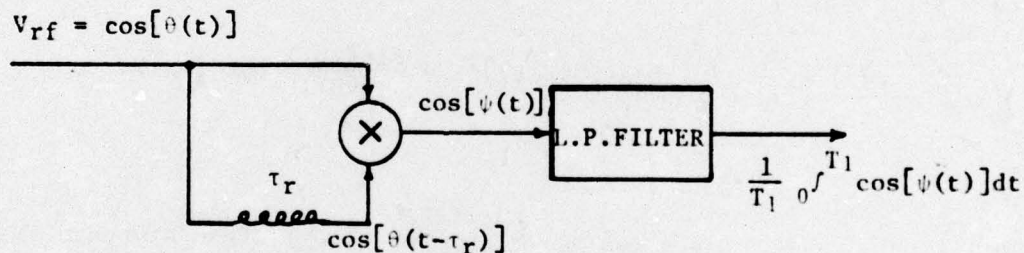


Figure A-1. Delay line correlator

Equation (A-1) may be evaluated by making a change in variable in the second integral. Letting $\zeta = \tau \omega_C(t')$, we have

$$\psi(t) = \tau_R \omega_C(t) - \omega_S \int_{\tau \omega_C(t - \tau_R)}^{\tau \omega_C(t)} \frac{\sin(\zeta)}{\tau \dot{\omega}(t')} d\zeta$$

Assuming that $\dot{\omega}(t')$ is constant with respect to ζ over the interval of integration, then

$$\psi(t) = \tau_R \omega_C(t) + \frac{\omega_S}{\tau \dot{\omega}(t')} \{ \cos[\tau \omega_C(t)] - \cos[\tau \omega_C(t - \tau_R)] \} \quad (A-2)$$

A Taylor series approximation for $c(t - \tau)$ is

$$\omega_c(t - \tau) \approx \omega_c(t) - \dot{\omega}_c(t)\tau$$

Using this approximation and noting that $\dot{\omega}(t') \approx \dot{\omega}(t)$, (A-2) becomes

$$\psi(t) = \tau \omega_c(t) + \frac{\omega_s}{\tau \dot{\omega}(t)} \{ \cos[\tau \omega_c(t)] - \cos[\tau \omega_c(t) - \tau \dot{\omega}_c(t)\tau] \}$$

Using a trigonometric identity, this reduces to

$$\psi(t) = \tau \omega_c(t) - \omega_s \tau \left(\frac{\sin \xi/2}{\xi/2} \right) \sin [\tau \omega_c(t) - \xi/2] \quad (A-3)$$

where $\xi \triangleq [\tau \dot{\omega}_c(t)]$.

For sawtooth FM, the sign of $\dot{\omega}(t)$ does not change and the doppler signal is obtained by time averaging $A_r \cos[\psi]$ over the modulation period T_1 . If this integration is carried out, where the phase $\xi/2$ in the $\sin[\tau \omega_c(t) - \xi/2]$ factor is set equal to zero, since it only effects the absolute doppler phase angle, we obtain

$$\frac{A_r}{T_1} \int_0^{T_1} \cos[\psi(t)] dt = A_r \rho(\tau) + \frac{A_r}{2} \omega_s \tau \left[\frac{\sin(\xi/2)}{\xi/2} \right] [\rho(\tau - \tau) - \rho(\tau + \tau)] \quad (A-4)$$

where

$$\rho(\tau) = \frac{1}{T_1} \int_0^{T_1} \cos[\tau \omega_c(t)] dt = \frac{\sin(\pi B \tau)}{(\pi B \tau)} \cos(\omega_0 \tau)$$

Here

$$\xi = \tau \dot{\omega}(t)\tau = \left[\frac{2\pi B \tau}{T_1} \right] \tau \triangleq \omega_r \tau \quad (\text{for sawtooth FM})$$

and $\omega_r \triangleq \dot{\omega}_c(t)\tau$ is the difference frequency caused by the mixing of the sawtooth FM oscillator RF signal with that of the delay line output. This result is the same as equation (20) but with an additional factor on the signal term of $\sin(\xi/2)/(\xi/2)$. A plot of this attenuation factor is shown in Figure A-2.

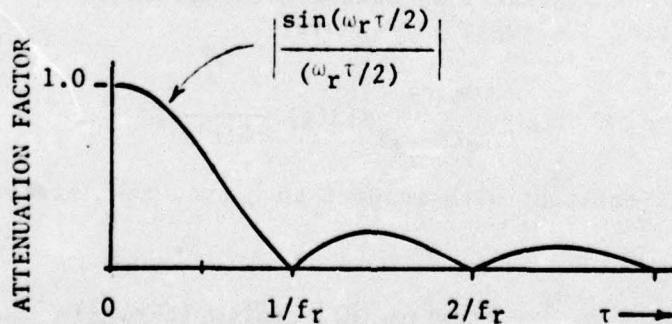


Figure A-2. Attenuation due to phase shift of oscillator reaction by delay line for sawtooth FM

If τ_r is too large this factor will cause the amplitude of the target signal correlation peak, which occurs at $\tau = \tau_r$ to decrease. The effect of this term is to reduce the correlation peak amplitude when the frequency, f_r , of the balanced mixer output is too high. For instance; if the reference delay time τ_r is equal to 0.50 μ sec, then the period of the sawtooth must be adjusted so that f_r is less than 1 MHz if the correlation peak at $\tau = \tau_r$ is not to be appreciably attenuated. This attenuation factor can be used to shape the side lobe range response, or to reduce the third harmonic response at $\tau = 3\tau_r$ when digital delay lines are used.

For triangular FM the effect of the additional factor occurs at shorter delay times. To derive this, we can use (A-3) as a starting point to get

$$\begin{aligned}\psi(t)_U &= \tau_r \omega_c(t) - \omega_s \tau_r \left(\frac{\sin \xi/2}{\xi/2} \right) \sin [\tau \omega_c(t) - (\xi/2)_U] , & 0 < t < T_1/2 \\ \psi(t)_D &= +\tau_r \omega_c(t) - \omega_s \tau_r \left(\frac{\sin \xi/2}{\xi/2} \right) \sin [\tau \omega_c(t) - (\xi/2)_D] , & T_1/2 < t < T_1\end{aligned}\tag{A-5}$$

where

$$(\xi)_U = [\tau_r \dot{\omega}(t)]_{U\tau} = -(\xi)_D$$

and the subscripts U or D indicate the relationship of the variable during the upswing or downswing times of the triangular modulation. Because the variable ξ changes sign on the downswing of the modulation, when we average $A_r \cos \psi(t)$ over the period of the modulation, T_1 , we now get

$$\begin{aligned}\frac{A_r}{T_1} \int_0^{T_1} \cos[\psi(t)] dt &= \frac{A_r}{T_1} \int_0^{T_1/2} \cos[\psi(t)_U] dt + \frac{A_r}{T_1} \int_{T_1/2}^{T_1} \cos[\psi(t)_D] dt \\ &= A_r \rho(\tau_r) + \frac{A_r}{2} \omega_s \tau_r \left(\frac{\sin \xi/2}{\xi/2} \right) \cos \xi/2 \frac{2}{T_1} \int_0^{T_1/2} \cos[\tau \omega_c(t)] dt \\ &= A_r \rho(\tau_r) + \frac{A_r}{2} \omega_s \tau_r \left(\frac{\sin \xi}{\xi} \right) [\rho(\tau - \tau_r) - \rho(\tau + \tau_r)]\end{aligned}\tag{A-6}$$

where

$$\rho(\tau) = \frac{1}{T_1} \int_0^{T_1} \cos[\tau \omega_c(t)] dt = \frac{\sin(\pi B \tau)}{(\pi B \tau)} \cos \omega_0 \tau$$

and

$$\xi = [\tau_r \dot{\omega}(t)]_{U\tau} = \left[\frac{4\pi B \tau_r}{T_1} \right] \tau = \omega_r \tau \quad (\text{for triangular FM}) .$$

This result, for triangular FM, produces an additional range attenuation, given by $\sin(\omega_r \tau) / (\omega_r \tau)$, which has a first null at $\tau = 1/2f_r$; whereas for sawtooth FM, the first null occurred at $\tau = 1/f_r$. Thus, for a given delay line and for a given percentage of attenuation due to this term, triangular FM requires that the reference beat frequency be one-half of that for sawtooth FM.

DISTRIBUTION LIST

U.S. Army Materiel Development
& Readiness Command
5001 Eisenhower Avenue
Alexandria, VA 22333
ATTN: DRCRD-BN
ATTN: DRCL

Defense Documentation Center
5010 Duke Street
Alexandria, VA 22314
ATTN: DDC-TCA (12 copies)

Harry Diamond Laboratories
2800 Powder Mill Road
Adelphi, MD 20783
ATTN: McGregor, Thomas, Commanding Officer
ATTN: Carter, W.W., Dr., Technical Director
ATTN: Associate Directors (1 copy)
ATTN: Chief, Lab 100
ATTN: Chief, Lab 200
ATTN: Chief, Lab 400
ATTN: Chief, Lab 500
ATTN: Chief, Lab 600
ATTN: Chief, Branch 140
ATTN: Record Copy, Branch 041
ATTN: Technical Reports, Branch 013
ATTN: HDL Library (3 copies)
ATTN: Chairman, HDL Editorial Committee, Branch 320